


Winter 2001

Mathematical Models of Quiescent Solar Prominences

Iain McKaig
Old Dominion University

Follow this and additional works at: https://digitalcommons.odu.edu/mathstat_etds

 Part of the [Astrophysics and Astronomy Commons](#), [Fluid Dynamics Commons](#), and the [Mathematics Commons](#)

Recommended Citation

McKaig, Iain. "Mathematical Models of Quiescent Solar Prominences" (2001). Doctor of Philosophy (PhD), dissertation, Mathematics and Statistics, Old Dominion University, DOI: 10.25777/dh52-5y22
https://digitalcommons.odu.edu/mathstat_etds/96

This Dissertation is brought to you for free and open access by the Mathematics & Statistics at ODU Digital Commons. It has been accepted for inclusion in Mathematics & Statistics Theses & Dissertations by an authorized administrator of ODU Digital Commons. For more information, please contact digitalcommons@odu.edu.

**MATHEMATICAL MODELS OF QUIESCENT SOLAR
PROMINENCES**

by

Iain McKaig
B.A., Virginia Wesleyan College, 1984
M.S., Old Dominion University, 1990

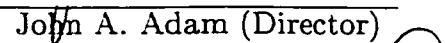
A Dissertation Submitted to the Faculty of
Old Dominion University in Partial Fulfillment of the
Requirements for the Degree of

DOCTOR OF PHILOSOPHY

COMPUTATIONAL AND APPLIED MATHEMATICS

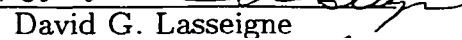
OLD DOMINION UNIVERSITY
December 2001


Approved by:


John A. Adam (Director)


Gary E. Copeland


John M. Dorrepaal


David G. Lasseigne


Stanley E. Weinstein

ABSTRACT

MATHEMATICAL MODELS OF QUIESCENT SOLAR PROMINENCES

Iain McKaig
Old Dominion University, 2001
Director: Dr. John A. Adam

Magnetic fields in the solar atmosphere suspend and insulate dense regions of cool plasma known as prominences. The convection zone may be the mechanism that both generates and expels this magnetic flux through the photosphere in order to make these formations possible. The connection is examined here by modeling the convection zone as both one-dimensional, then more realistically, two-dimensional.

First a Dirichlet problem on a semi-infinite strip is solved using conformal mapping and the method of images. The base of the strip represents the photosphere where a current distribution can be given as a boundary condition, and the strip extends into a current free atmosphere. Secondly a diffusion equation with convection terms is assigned to a two-dimensional region below the photosphere to represent the convection zone, and this is matched to Laplace's equation above the photosphere to represent the corona. The PDE's are solved numerically to find the magnetic field lines.

In both cases the solutions obtained resemble classic magnetic topologies that have been used to model quiescent prominences. Some of the solutions even have the feet observed to drop into supergranule boundaries.

Dedicated

to

Charles and Joyce McKaig.

Both deserve a Ph.D. in parenting

ACKNOWLEDGMENTS

I would like to thank the members of my committee for all their advice, suggested improvements to this dissertation, and ideas for future work. I owe a special debt of gratitude to Dr. Adam, not only for convincing me to come back to graduate school, but for all his encouraging words. My exploration into magnetohydrodynamics would have been exponentially harder without his advice and support.

My wife, Judy, also deserves appreciation, not only for her patience and support, but for her tireless reading of this manuscript. Her understanding was more valuable than she will ever know.

TABLE OF CONTENTS

| | | |
|----------|--|-----------|
| 1 | Introduction | 1 |
| 2 | Magnetohydrodynamics | 11 |
| 2.1 | The Basic Equations of MHD | 12 |
| 2.1.1 | The Fluid Equations | 12 |
| 2.1.2 | The Electromagnetic Equations | 14 |
| 2.2 | The Induction Equation | 16 |
| 2.2.1 | The Diffusive Limit | 17 |
| 2.2.2 | The Perfectly Conducting Limit and the Frozen Flux Theorem | 17 |
| 2.3 | The Lorentz Force | 18 |
| 2.4 | Energy Considerations | 19 |
| 2.5 | Summary of Equations | 20 |
| 2.6 | Flux Tubes and Current Sheets | 21 |
| 2.6.1 | Flux Tubes | 21 |
| 2.6.2 | Current Sheets | 23 |
| 2.7 | Magnetohydrostatics | 23 |
| 2.7.1 | The Plasma Beta | 26 |
| 2.7.2 | Potential Fields | 26 |
| 2.7.3 | Force-Free Fields | 26 |
| 2.7.4 | Magnetohydrostatics and Flux Tubes | 27 |

| | | |
|----------|---|-----------|
| 2.8 | Waves | 28 |
| 2.8.1 | Sound Waves | 30 |
| 2.8.2 | Alfvén Waves | 31 |
| 2.8.3 | Gravity Waves | 33 |
| 2.8.4 | Magnetoacoustic Waves | 36 |
| 2.8.5 | Acoustic-Gravity Waves | 37 |
| 2.8.6 | Magnetoacoustic-Gravity Waves | 39 |
| 2.9 | MHD Instabilities | 40 |
| 3 | A History of Prominence Models and Magnetoconvection | 43 |
| 3.1 | A History of Prominence Models | 43 |
| 3.1.1 | The Early Models of Menzel and Dungey | 49 |
| 3.1.2 | The Kippenhahn-Schlüter Model | 50 |
| 3.1.3 | Kuperus-Raadu Model | 52 |
| 3.2 | Magnetoconvection | 55 |
| 4 | Solar Prominence Magnetic Configurations and Convection | 59 |
| 4.1 | A Dirichlet Problem with Applications to Solar Prominences | 59 |
| 4.2 | Solar Prominence Magnetic Configurations Derived Numerically from Convection | 62 |
| 5 | Conclusion | 86 |
| | Bibliography | 88 |

| | |
|---|------------|
| Appendices | 94 |
| A The Method of Images | 94 |
| B The Mathematica Code | 96 |
| C Permission to use Copyrighted Material | 101 |
| Vita | 105 |

LIST OF FIGURES

| | | |
|-----|--|----|
| 1.1 | The various layers of the Sun together with some surface and atmospheric features. | 3 |
| 1.2 | A sunspot surrounded by granulation cells. | 8 |
| 1.3 | Magnetic flux escaping the surface of the Sun. | 9 |
| 1.4 | A large sunspot group. | 9 |
| 1.5 | Helmet streamers (right/left) and coronal holes (top/bottom). | 10 |
| 1.6 | Two coronal mass ejections on opposite sides of the Sun. | 10 |
| 2.1 | A Flux Tube. | 25 |
| 2.2 | ds and dz on a field line. | 25 |
| 2.3 | A polar diagram for shear (solid) and compressional (dashed) Alfvén waves. | 34 |
| 2.4 | A rising parcel of fluid. | 34 |
| 2.5 | Polar diagram for fast (dashed) and slow (solid) magnetoacoustic waves. | 38 |
| 2.6 | $\omega - k_x$ diagnostic diagram. | 42 |
| 3.1 | A prominence seen on the limb of the Sun. | 45 |
| 3.2 | Filaments seen against the surface of the Sun. | 45 |
| 3.3 | An eclipse photograph showing helmet streamers and coronal cavities above solar prominences. | 46 |
| 3.4 | A sequence of photographs showing a coronal mass ejection. | 46 |
| 3.5 | A representative plasma sheet suspended above the photosphere. | 48 |

| | | |
|------|---|----|
| 3.6 | Typical field lines of the KS (left) and KR (right) models, anchored to the photosphere. | 48 |
| 3.7 | Field lines of Menzel's model. | 51 |
| 3.8 | Field lines of Dungey's model. | 51 |
| 3.9 | Field lines of the Kippenhahn-Schlüter model. | 54 |
| 3.10 | The Kuperus-Raadu magnetic configuration. | 54 |
| 3.11 | One of Parker's solutions to the steady state induction equation. . . . | 57 |
| 3.12 | The expulsion of magnetic flux from a convection cell. | 58 |
| 4.1 | The xy and uv planes. | 63 |
| 4.2 | $f(x) = 1$ and $g(y) = 0$ | 63 |
| 4.3 | $f(x) = \sin x $ and $g(y) = 0$ | 64 |
| 4.4 | $f(x) = \cos x$ and $g(y) = 0$ | 64 |
| 4.5 | $f(x) = \sin x $ and $g(y) = 1$ if $0 < y < .5$, 0 if $y > .5$ | 65 |
| 4.6 | $f(x) = 1$ and $g(y) = 1$ if $0 < y < .5$, 0 if $y > .5$ | 65 |
| 4.7 | The xy -plane. | 66 |
| 4.8 | The stream function $\Psi_1(x, y) = -\sin x \sinh y$. A deep convection cell with a downflow at the center. | 71 |
| 4.9 | The stream function $\Psi_2(x, y) = -e^{-y} \sin x$. A deep convection cell with an upflow in the center. | 71 |
| 4.10 | The stream function Ψ_1 (light lines) and the magnetic field lines with $g1(y) = g2(y) = 0$ and $h1(x) = 0, h2(x) = 100$ | 72 |

| | | |
|------|---|----|
| 4.11 | The stream function Ψ_1 (light lines) and the magnetic field lines with $g1(y) = g2(y) = 0$ and $h1(x) = 100, h2(x) = 0$ | 72 |
| 4.12 | The stream function Ψ_1 (light lines) and the magnetic field lines with $g1(y) = g2(y) = 0$ and $h1(x) = 100, h2(x) = 100$ | 73 |
| 4.13 | The stream function Ψ_1 (light lines) and the magnetic field lines with $g1(y) = g2(y) = 100$ and $h1(x) = 0, h2(x) = 0$ | 73 |
| 4.14 | The stream function Ψ_1 (light lines) and the magnetic field lines with $g1(y) = g2(y) = 100$ and $h1(x) = 0, h2(x) = 100$ | 74 |
| 4.15 | The stream function Ψ_1 (light lines) and the magnetic field lines with $g1(y) = g2(y) = 100$ and $h1(x) = 100, h2(x) = 0$ | 74 |
| 4.16 | The stream function Ψ_1 (light lines) and the magnetic field lines with $g1(y) = g2(y) = 100$ and $h1(x) = 100, h2(x) = 100$ | 75 |
| 4.17 | The stream function Ψ_1 (light lines) and the magnetic field lines with $g1(y) = g2(y) = 100$ if $y < 0, 0$ if $y > 0$ and $h1(x) = 0, h2(x) = 0$. . . | 75 |
| 4.18 | The stream function Ψ_1 (light lines) and the magnetic field lines with $g1(y) = g2(y) = 100$ if $y < 0, 0$ if $y > 0$ and $h1(x) = 0, h2(x) = 100$. . | 76 |
| 4.19 | The stream function Ψ_1 (light lines) and the magnetic field lines with $g1(y) = g2(y) = 100$ if $y < 0, 0$ if $y > 0$ and $h1(x) = 100, h2(x) = 0$. . | 77 |
| 4.20 | The stream function Ψ_1 (light lines) and the magnetic field lines with $g1(y) = g2(y) = 100$ if $y < 0, 0$ if $y > 0$ and $h1(x) = 100, h2(x) = 100$ | 78 |
| 4.21 | The stream function Ψ_2 (light lines) and the magnetic field lines with $g1(y) = g2(y) = 0$ and $h1(x) = 0, h2(x) = 100$ | 79 |

| | | |
|------|---|----|
| 4.22 | The stream function Ψ_2 (light lines) and the magnetic field lines with $g_1(y) = g_2(y) = 0$ and $h_1(x) = 100, h_2(x) = 0$ | 79 |
| 4.23 | The stream function Ψ_2 (light lines) and the magnetic field lines with $g_1(y) = g_2(y) = 0$ and $h_1(x) = 100, h_2(x) = 100$ | 80 |
| 4.24 | The stream function Ψ_2 (light lines) and the magnetic field lines with $g_1(y) = g_2(y) = 100$ and $h_1(x) = 0, h_2(x) = 0$ | 80 |
| 4.25 | The stream function Ψ_2 (light lines) and the magnetic field lines with $g_1(y) = g_2(y) = 100$ and $h_1(x) = 0, h_2(x) = 100$ | 81 |
| 4.26 | The stream function Ψ_2 (light lines) and the magnetic field lines with $g_1(y) = g_2(y) = 100$ and $h_1(x) = 100, h_2(x) = 0$ | 81 |
| 4.27 | The stream function Ψ_2 (light lines) and the magnetic field lines with $g_1(y) = g_2(y) = 100$ and $h_1(x) = 100, h_2(x) = 100$ | 82 |
| 4.28 | The stream function Ψ_2 (light lines) and the magnetic field lines with $g_1(y) = g_2(y) = 100$ if $y < 0, 0$ if $y > 0$ and $h_1(x) = 0, h_2(x) = 0$. . . | 82 |
| 4.29 | The stream function Ψ_2 (light lines) and the magnetic field lines with $g_1(y) = g_2(y) = 100$ if $y < 0, 0$ if $y > 0$ and $h_1(x) = 0, h_2(x) = 100$. . | 83 |
| 4.30 | The stream function Ψ_2 (light lines) and the magnetic field lines with $g_1(y) = g_2(y) = 100$ if $y < 0, 0$ if $y > 0$ and $h_1(x) = 100, h_2(x) = 0$. . | 84 |
| 4.31 | The stream function Ψ_2 (light lines) and the magnetic field lines with $g_1(y) = g_2(y) = 100$ if $y < 0, 0$ if $y > 0$ and $h_1(x) = 100, h_2(x) = 100$ | 85 |

CHAPTER 1

INTRODUCTION

If the Sun had no magnetic field, then it would be as boring as most astronomers think it is. *R.B. Leighton*

This thesis[†] is concerned with modeling a specific formation of plasma that can be observed in the corona, or atmosphere, of the Sun – quiescent prominences. The magnetic fields that create and support these structures are presumably generated in the convection zone below the visible surface. This chapter is offered as a brief introduction to solar structure so the reader can better understand the regions under discussion. Subsequent chapters will review the mathematics needed to describe the interaction of magnetism and electrically charged fluids, present a history of prominence models, and introduce new models created to tie together the expulsion of magnetic flux by convection to the support of prominences in the solar atmosphere.

To a first approximation the Sun can be thought of as a ball of hot plasma formed by the gravitational collapse of a primordial cloud of hydrogen gas. Once the internal pressure and temperature became high enough nuclear reactions could begin to provide an outward force to balance the inward force of gravity. The resulting ball of plasma, in hydrothermal equilibrium, is layered like an onion into regions defined by the most dominant form of energy transport (see figure 1.1). This picture is compli-

[†]The Model Journal used for this dissertation is *Wave Motion*.

cated though by rotation and magnetism, effects that give rise to interesting features in the surface and above.

The Sun is roughly divided into two basic regions, the interior that lies below the photosphere (the visible surface of the Sun) and the exterior atmosphere above – but even these regions are further subdivided. The former is divided into the core, radiative zone and the convection zone.

THE CORE: The pressure in the core is high enough for nuclear fusion (through several intermediate steps) to convert four hydrogen nuclei (protons) into a helium ion (two protons and two neutrons). The helium ion is 3% less massive than the protons and the resulting mass loss is converted into energy ($E = mc^2$) that escapes in the form of high energy photons (gamma rays). As the photons move away from the core they are continually absorbed and emitted by electrons as they go. It can take up to the order of 10 000 years for a photon to reach the surface; its energy reduced to that of visible light by this time. This defines the photosphere. The core takes up about 25% of the Sun's radius and has a density ranging from 10 times that of lead in the very center to approximately equal to lead at the edge of the core. The central core temperature is about 10^7 K and 7×10^6 K at the boundary.

THE RADIATIVE ZONE: In this region the pressure is not high enough for nuclear reactions to occur but it is still too hot for protons to capture free electrons. Heat energy rises to the surface by radiation. This zone extends to 70% of the Sun's radius and the temperature drops slowly from about 7×10^6 K to 2×10^6 K. The density of the radiative zone is about a fifth that of water.

THE CONVECTION ZONE: In the convection zone the temperature becomes low

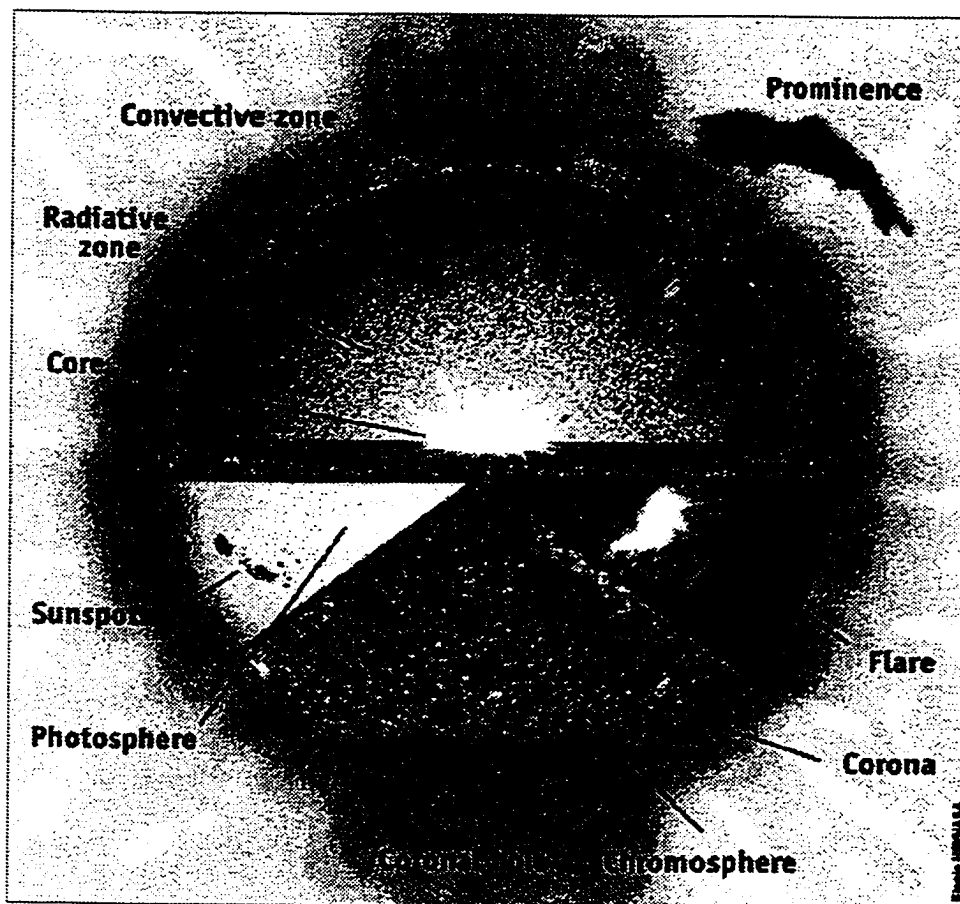


Fig. 1.1: The various layers of the Sun together with some surface and atmospheric features.

courtesy SOHO/EIT consortium, a project of NASA and ESA

enough for ions to trap electrons increasing the opacity (the ability of a material to transmit photons) of the gas. This slows the transport of radiation and the gas now starts absorbing heat so the dominant energy transportation method becomes convection. Hot cells of plasma expand and become buoyant, rising to the surface then cooling and sinking to pick up more heat. The tops of the convection cells can be seen at the surface as supergranules that are about 30 000 km across and on a smaller scale as granules (see figure 1.2) approximately 1000 km across. The temperature drops to about 6600 K at the surface where the density has fallen to less than that of air at sea level.

The Sun's magnetic field is thought to be generated at the border of the radiative and convection zones. The high shearing of the plasma's velocity field stretches and twists the magnetic field lines making them stronger (this is the mechanism associated with the so called "solar dynamo"). The convection then carries field to the surface where it emerges to shape the surrounding material into many types of interesting phenomena (see figure 1.3).

The flow in the convection zone is not just outward. Since the Sun is a ball of gas it does not rotate as a rigid body and convection cells are sheared by differential rotation. It takes the Sun about 27 days to rotate at the equator and 37 days near the pole. Buoyancy also drives a weak equator-to-pole flow known as meridional flow. Acoustic waves generated in the convection zone resonate through the interior provide information used to study stellar structure [1, 2].

The exterior atmosphere of the Sun is usually divided into the photosphere, chromosphere and the corona, although there is a thin region below the corona known as

the transition zone. It is in the atmosphere that the plasma pressure drops so the magnetic field can move and structure the gas.

THE PHOTOSPHERE: This is the visible surface of the Sun where the energy of the photons generated in the core has been reduced to that of visible light. The magnetic field escaping the convection zone creates many types of formations on and above the photosphere: sunspots, flares, spicules, prominences, etc. *Sunspots* are regions of an intense and organized magnetic field that insulate the gas from its surroundings so the sunspot has a temperature of approximately 1000 K less than the rest of the photosphere. Lasting from days to months they form near mid latitudes and drift towards the equator (see figures 1.2 and 1.4). Sound waves have been observed resonating through sunspots [3]. *Flares* can erupt suddenly near sunspots, ejecting material into the atmosphere above. *Spicules* are columns of plasma that form at the edge of supergranule boundaries where 90% of the surface magnetic field is concentrated. They rise suddenly into the chromosphere at 20–30 km/s but are not observed falling back, the gas presumably becoming part of the corona or the solar wind – a stream of gas and ions flowing away from the Sun. The photosphere is also structured by acoustic waves that propagate through the convection zone. Doppler shifts in the velocity of the photospheric gas can be inverted to provide information about the interior structure.

THE CHROMOSPHERE: This is an irregular layer that is structured by tangled magnetic field lines. The temperature rises from about 6000 K to 20 000 K but is extremely dependent on the local magnetic field configuration. In a thin region at the top of the chromosphere known as the transition zone the temperature rises from

20 000 K to 1 000 000 K over a distance of ≤ 100 km. The cause of this temperature increase is an active area of research.

THE CORONA: The corona is the true atmosphere of the Sun and extends past the earth and outer planets to the heliopause where the Sun's magnetic field meets the intergalactic field. Visible close to the Sun as light scattered by dust and stray electrons, the gas is often organized into helmet streamers, tall columns of gas shaped by closed field lines that connect active regions on the surface (usually sunspots) that taper off at the end, and coronal holes, regions composed of open field lines where the plasma can escape to become part of the solar wind (see figure 1.5). The structure of the corona changes slowly with the 11 year magnetic cycle, but sudden events known as coronal mass ejections can occur (see figure 1.6). Over a period of hours plasma caught in closed field lines is ejected into interplanetary space. These storms can effect the earth causing power failures and damage to satellites. A resource for pictures of the solar surface and atmosphere is the website of SOHO, the SOLar and Heliospheric Observatory, at <http://sohowww.nascom.nasa.gov/>. This is a satellite that monitors the Sun continuously with various instruments.

It is clear that the Sun is a complicated object, ripe for many applications of techniques in mathematical physics. Since the magnetic field plays a major role in how the fluid flows it is necessary to introduce the subject of magnetohydrodynamics (MHD). This is surveyed in the next chapter. This outline of MHD comes from three sources: Cosmical Magnetic fields - their origin and activity, a monumental work by E.N. Parker [4], Solar Magnetohydrodynamics by E.R. Priest [5], a useful compendium wherein MHD theory is applied to the Sun, and the classic work that

started the field, Magnetohydrodynamics by T.G. Cowling [6].

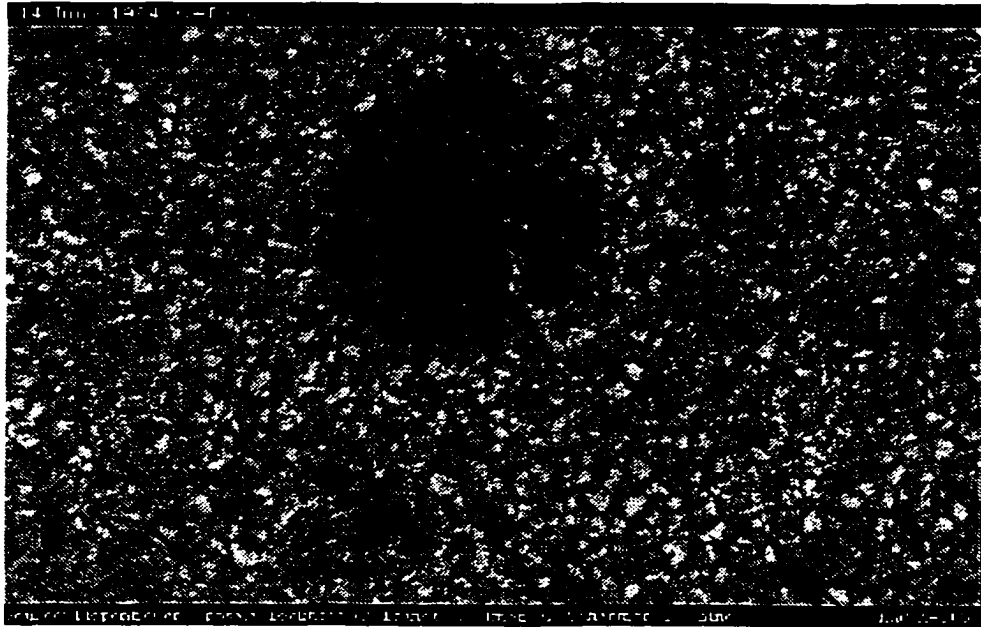


Fig. 1.2: A sunspot surrounded by granulation cells.

courtesy of the High Altitude Observatory/NCAR



Fig. 1.3: Magnetic flux escaping the surface of the Sun.

courtesy SOHO/EIT consortium, a project of NASA and ESA

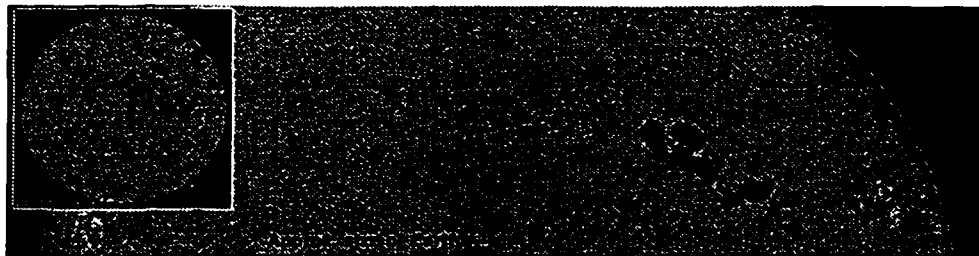


Fig. 1.4: A large sunspot group. With an area of more than 13 times the surface of the earth this group was responsible for many flares and coronal mass ejections.

courtesy SOHO/EIT consortium, a project of NASA and ESA

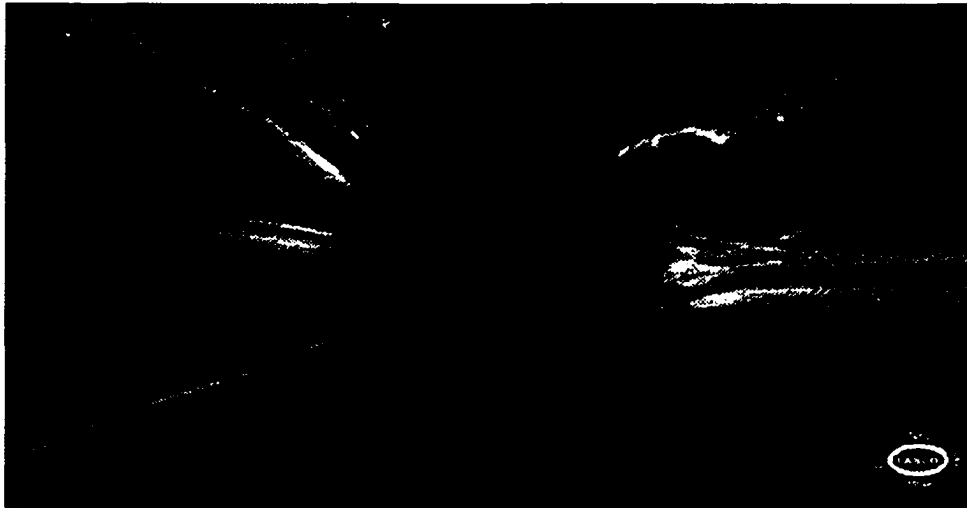


Fig. 1.5: Helmet streamers (right/left) and coronal holes (top/bottom).

courtesy SOHO/EIT consortium, a project of NASA and ESA

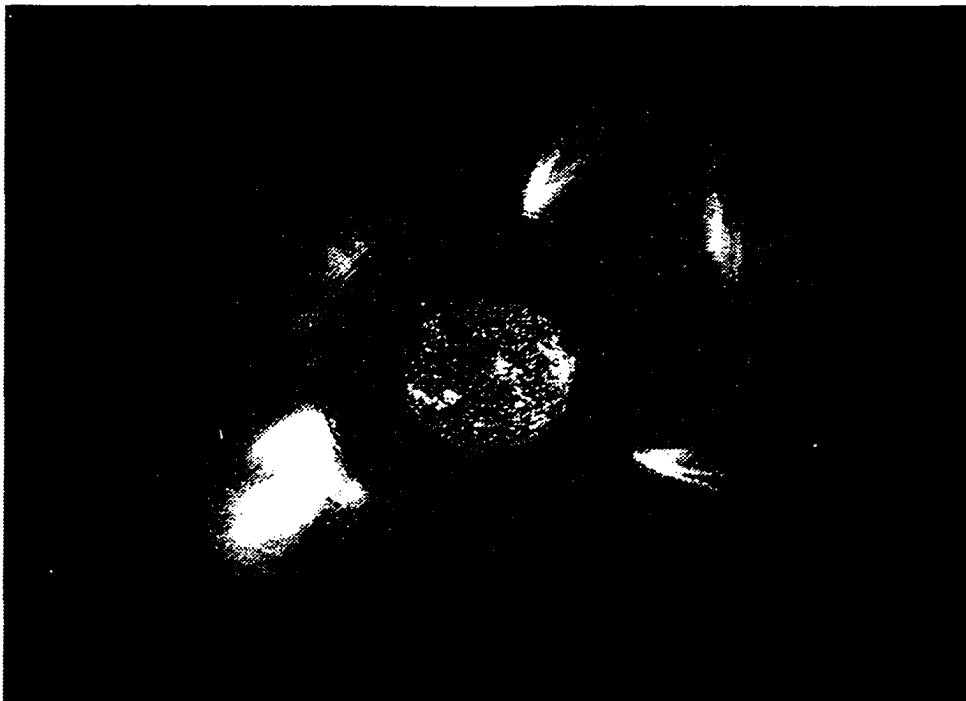


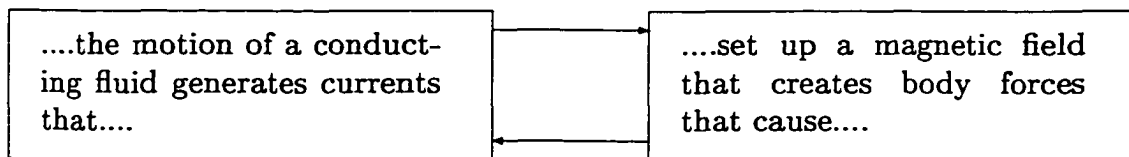
Fig. 1.6: Two coronal mass ejections on opposite sides of the Sun.

courtesy SOHO/EIT consortium, a project of NASA and ESA

CHAPTER 2

MAGNETOHYDRODYNAMICS

Magnetohydrodynamics (MHD) is the branch of fluid dynamics concerned with the motion of an electrically conducting fluid in an electromagnetic field. The charges in the fluid, when set in motion, create a magnetic field which can then influence the motion of the fluid itself. Charge densities external to the fluid can also affect (and be affected by) the motion of the fluid. Thus there is a coupled system of fields and bulk motion of matter.



In MHD the fluid is often called a plasma, but an important distinction has to be made. In plasmas the charges (usually electrons) have room to be accelerated by the field between atomic collisions. The electrons and positive ions can become separated, creating strong electrostatic restoring forces (the cause of plasma waves); electrical conductivity becomes important and particle velocities can become a significant percentage of the speed of light (c). A particle / statistical approach has to be used (using Boltzmann's equation) and relativistic effects have to be considered. In MHD the fluid (which could be a dense ionized gas) has no significant separation of charge, the collision frequency is high, and a continuum approach can be used. The

velocity of a parcel of fluid satisfies $v \ll c$ so relativistic effects can be ignored. MHD waves are the low-frequency counterpart of plasma waves.

So, in MHD a fluid element is not only acted upon by the usual hydrodynamic forces of viscosity, buoyancy and gravity, but also by an electromagnetic (Lorentz) force. As the element moves it changes the distribution of charge, hence changing the field. This added electromagnetic force can impart elastic properties to the fluid bringing in new modes of wave propagation to transmit fluid properties around the domain of interest. The governing equations of MHD are a union of Maxwell's equations and the usual fluid equations.

2.1 The Basic Equations of MHD

2.1.1 The Fluid Equations

The fluid equations consist of a continuity equation and an equation of motion in addition to an energy equation and an equation of state. They couple together the primary variables ρ (the matter density), \vec{v} (the fluid velocity field) and p (the fluid pressure). All dependent variables are functions of space and time, and are given in SI (MKS) units. The equations are:

The Continuity Equation:

$$\frac{\partial \rho}{\partial t} + \nabla \cdot (\rho \vec{v}) = 0,$$

expresses the fact that matter can neither be created nor destroyed. If the density is increasing in time then the mass flux must be negative, and vice versa.

The Equation of Motion:

$$\rho \frac{D\vec{v}}{Dt} = -\nabla p + \vec{j} \times \vec{B} + \rho \vec{g} + \rho \nu \nabla^2 \vec{v},$$

is essentially Newton's second law of motion. $\frac{D}{Dt} = \frac{\partial}{\partial t} + (\vec{v} \cdot \nabla)$ is the material (or convective) derivative. The forces included here are the pressure, the Lorentz force (mentioned above but to be explained later in section 2.3), gravity, and the viscous force for an incompressible fluid. The Lorentz force is electromagnetic in origin and couples the fluid equations with the electromagnetic equations (section 2.1.2). ν is the coefficient of kinematic viscosity. The viscous force term becomes more complicated for a compressible fluid. More force terms can be added as needed for more involved situations (for example, if the rotation of the fluid is taken into account by moving to a frame of reference with an angular velocity). Also, force terms can be neglected to obtain approximate solutions. It is common, for example, to neglect gravity when the maximum length scale of a model is less than the scale height, $H = \left(-\frac{1}{p} \frac{dp}{dz}\right)^{-1}$ for a stable atmosphere (the height over which the pressure varies by a factor of e).

The Energy Equation:

$$\rho T \frac{Ds}{Dt} = -L,$$

is presented here in a very basic form. L is the energy loss function, s is the entropy per unit mass of the fluid, and T is the temperature. This equation expresses the fact that any increase in heat energy per unit volume as a fluid element moves around a domain is due to energy sources or sinks as reflected in L . Note that $L = 0$ corresponds to the constant entropy case. This equation can be written in a myriad of forms depending on the sources of energy considered important and will be discussed more fully in

section 2.4.

The Equation of State:

$$p = \frac{1}{\bar{\mu}} \rho R T,$$

is the ideal gas law. R is the gas constant, and $\bar{\mu}$ is the mean atomic weight (usually set to $\frac{1}{2}$ due to the abundance of Hydrogen). This equation can also take on different forms depending on the physical properties of the domain.

2.1.2 The Electromagnetic Equations

These are the empirically-derived Maxwell equations and Ohm's law. They link the values of \vec{B} (the magnetic induction, often called the magnetic field), \vec{E} (the electric field) and \vec{j} (the current density). All are also given in SI units and are functions of space and time. Maxwell's equations consist of Ampere's equation, Faraday's equation, the solenoidal condition, and a charge conservation law.

Ampere's Equation:

$$\nabla \times \vec{B} = \mu \vec{j} + \frac{1}{c^2} \frac{\partial \vec{E}}{\partial t},$$

where μ is the magnetic permeability, states that currents or time-varying electric fields can create a magnetic field.

Faraday's Equation:

$$\nabla \times \vec{E} = -\frac{\partial \vec{B}}{\partial t},$$

expresses the observation that time-varying magnetic fields can create an electric field.

The Solenoidal Condition:

$$\nabla \cdot \vec{B} = 0,$$

“prevents” the existence of sources or sinks of magnetic fields. Lines of constant magnetic field must form closed loops.

Charge Conservation:

$$\nabla \cdot \vec{E} = \frac{\rho^*}{\epsilon},$$

where ρ^* is the charge density and ϵ is the permittivity of free space (note that $c = (\mu\epsilon)^{-\frac{1}{2}}$), shows that charges create electric fields.

In solar MHD the last term in Ampere’s equation (called the displacement current), so ingeniously added by Maxwell to create the equations named after him, is ignored. The reason is as follows:

Let L and T be length and time scales, so $V = L/T$ is a characteristic velocity scale. Also let B and E be characteristic values for the magnetic and electric fields. Faraday’s equation $\Rightarrow \frac{E}{L} \approx \frac{B}{T}$ so $E \approx VB$, $\Rightarrow \frac{1}{c^2} \frac{\partial \vec{E}}{\partial t} \approx \frac{1}{c^2} \frac{E}{T} = \frac{B}{L} \frac{V^2}{c^2}$. Now $\nabla \times \vec{B} \approx \frac{B}{L}$ so if $V \ll c$ then $\frac{1}{c^2} \frac{\partial \vec{E}}{\partial t} \ll \nabla \times \vec{B}$ thus the displacement current can be neglected.

Note that when this term is neglected Ampere’s equation $\Rightarrow \nabla \cdot \vec{j} = 0$, so accumulations of charge are negligible and currents flow in closed loops.

Ohms Law:

$$\vec{j} = \sigma(\vec{E} + \vec{v} \times \vec{B}),$$

is the final electromagnetic equation and links (through \vec{v}) these equations to those of the fluid. σ is the electrical conductivity. This is the usual Ohm’s law $j = \sigma E$ generalized to a moving conductor (which generates a magnetic field). Note that in the infinite conductivity limit this becomes $\vec{E} + \vec{v} \times \vec{B} = \vec{0}$.

In most solar MHD problems Ampere's equation, Faraday's equation, Ohm's law and the solenoidal condition are all used to get one equation involving just \vec{B} and \vec{v} . This is called the induction equation and can be used to explore some wide ranging properties of solar plasmas.

2.2 The Induction Equation

Ampere's equation (without the displacement current) and Ohm's law can be combined to eliminate \vec{j} , the current density. This gives $\vec{E} = \frac{1}{\mu\sigma}\nabla \times \vec{B} - \vec{v} \times \vec{B}$. Substitute this expression for \vec{E} into Faraday's equation, and let $\eta = \frac{1}{\mu\sigma}$ (the magnetic diffusivity) to find $\eta\nabla \times \nabla \times \vec{B} - \nabla \times \vec{v} \times \vec{B} = -\frac{\partial \vec{B}}{\partial t}$. Next use the solenoidal condition $\nabla \cdot \vec{B} = 0$ with the vector identity $\nabla \times \nabla \times \vec{B} = \nabla(\nabla \cdot \vec{B}) - \nabla^2 \vec{B}$ to obtain:

The Induction Equation:

$$\frac{\partial \vec{B}}{\partial t} = \nabla \times (\vec{v} \times \vec{B}) + \eta \nabla^2 \vec{B},$$

one equation connecting the fluid velocity and the magnetic field. Therefore in solar MHD, the only primary electromagnetic variable used is the magnetic field \vec{B} . Once the magnetic field is found, Ampere's equation gives the current density and Ohm's law can be used to find the electric field. The induction equation can be used to illustrate some consequences of combining magnetic fields with conducting fluids. Mathematically, both terms on the right hand side behave completely differently. The first term is convective while the second is diffusive – each can be dominant on different time and length scales. The convective term has a time scale of $T_{motion} = L/V$ while the diffusion term operates on a time scale $T_{diffusion} = L^2/\eta$. The ratio of

these time scales is a non-dimensional number called the magnetic Reynolds number $R_m = \frac{T_{diffusion}}{T_{motion}} = \frac{LV}{\eta}$. If $R_m \ll 1$ the diffusion dominates and if $R_m \gg 1$ convection dominates. Consider the consequences of each approximation.

2.2.1 The Diffusive Limit

If $R_m \ll 1$ (so $T_{diffusion} \ll T_{motion}$) then the induction equation reduces to the diffusion equation $\frac{\partial \vec{B}}{\partial t} = \eta \nabla^2 \vec{B}$ making the coupling between \vec{v} and \vec{B} very weak (note that this is also the case if $\vec{v} \equiv \vec{0}$). The magnetic field is free to spread through the fluid and any initially convoluted field will smooth out and decay over a time scale of $T_{diffusion} = L^2/\eta$. The energy in the magnetic field is converted to heat. This is known as ohmic dissipation. However, in most solar applications the length scale is large making this approximation invalid. For example, the magnetic field of a typical sunspot has a diffusion time of ≈ 300 years, but sunspots develop and fade over a matter of weeks.

2.2.2 The Perfectly Conducting Limit and the Frozen Flux Theorem

If $R_m \gg 1$ (so $T_{diffusion} \gg T_{motion}$) then an appropriate approximation for the induction equation is the transport type equation $\frac{\partial \vec{B}}{\partial t} = \nabla \times (\vec{v} \times \vec{B})$. The fluid velocity and the magnetic field are tied together and the magnetic field can no longer diffuse freely through the fluid. This is often called the perfectly conducting limit because if $T_{diffusion}$ dominates then η must be small so σ must be large. However, the electrical

conductivity varies little over large domains in the solar atmosphere so it has been suggested [5] that a better title should be the large length scale approximation. Note that this is the equation satisfied by the vorticity field in non-viscous fluid dynamics, with $\vec{B} = \vec{\omega}$ (not an exact analogy since $\vec{B} \neq \nabla \times \vec{v}$), and since vortex lines move with a fluid (the vorticity theorem of Helmholtz and Kelvin) then maybe lines of magnetic field do too. This is the case and the result is known as the frozen-flux theorem of Alfvén [6]:

In a perfectly conducting fluid ($R_m \rightarrow \infty$) magnetic field lines move with the fluid. i.e. the field lines are “frozen” into the plasma.

The proof involves showing that if $\Phi = \iint_S \vec{B} \cdot d\vec{S}$ (the total magnetic flux through a surface S) then $\frac{D\Phi}{Dt} = 0$. The flux through S as the surface moves about the fluid remains constant in time.

2.3 The Lorentz Force

The fluid velocity in Ohm’s law couples the electromagnetic equations to the fluid equations and the $\vec{j} \times \vec{B}$ term in the equation of motion connects the fluid equations to the electromagnetic ones. This force term is known as the Lorentz force and only has an effect on the fluid perpendicular to \vec{B} , and does not contribute parallel to \vec{B} . Any variation in fluid properties along the magnetic field lines must be due to hydrodynamic forces (such as gravity or a pressure gradient) only.

Using Ampere’s equation and a vector identity and writing the first term of the

result in a Frenet frame of reference, we can write the Lorentz force as:

$$\vec{j} \times \vec{B} = \frac{1}{\mu} (\nabla \times \vec{B}) \times \vec{B} = \frac{1}{\mu} (\vec{B} \cdot \nabla) \vec{B} - \nabla \left(\frac{B^2}{2\mu} \right) = \frac{B^2 K}{\mu} \hat{N} + \frac{d}{ds} \left(\frac{B^2}{2\mu} \right) \hat{T} - \nabla \left(\frac{B^2}{2\mu} \right),$$

where K is the curvature of the field line, s is the arc-length parameter, and \hat{N} and \hat{T} are unit normal and tangent vectors to the field line. This shows that the Lorentz force contributes a tension, of magnitude $\frac{B^2}{\mu}$, along the field lines directly proportional to how much the field lines curve, and an isotropic pressure force of magnitude $\frac{B^2}{2\mu}$. So the Lorentz force can be thought of as a magnetic tension along the field lines and a magnetic pressure in all directions. Lines of magnetic flux therefore have elastic properties and push against each other, achieving equilibrium only when these forces balance. These properties of the field lines suggest that they can support wave motion, dragging the fluid with them if the conductivity is high.

2.4 Energy Considerations

The energy equation $\rho T \frac{Ds}{Dt} = -L$ mentioned above is very general, but by using the equation of state for an ideal gas, and the fact that $s \propto \ln \left(\frac{p}{\rho^\gamma} \right)$ where γ is the ratio of specific heats, it can be put into the form $\frac{\rho}{\gamma-1} \frac{D}{Dt} \left(\frac{p}{\rho^\gamma} \right) = -L$. The decision to be made next is what sources and/or sinks of energy to include in L , the energy loss function. In the solar atmosphere the dominant energy transport mechanisms are thermal conduction, radiation and heating. To account for these mechanisms, L can be taken as:

$$L = -\nabla \cdot (\kappa \nabla T) + \rho^2 Q(T) - H.$$

The first term is for thermal conduction and κ is the anisotropic thermal conductivity tensor. The second term accounts for energy losses by plasma radiation. $Q(T)$ is the radiative loss function and is usually approximated by a piecewise continuous function of the form $Q(T) = \chi T^\alpha$ where χ and α are constant over various temperature ranges. The last term accounts for all the other sources of heating in the atmosphere – for example; heating due to the magnetic field, large scale currents (called ohmic heating), viscous heating, or mechanical heating by dissipation of acoustic waves.

However, when dealing with wave motions that act on a short enough time scale, we can neglect all these terms and set $L = 0$. A typical fluid element, when displaced by wave motions, will not have time to be acted on by any of these elements before the restoring forces act to displace the parcel once more. This is the adiabatic approximation which $\Rightarrow \frac{p}{\rho^\gamma}$ is constant. Using the continuity equation, the adiabatic form of the energy equation becomes:

$$\frac{\partial p}{\partial t} + \vec{v} \cdot \nabla p + \gamma p \nabla \cdot \vec{v} = 0.$$

2.5 Summary of Equations

The fundamental equations of MHD are:

The Continuity Equation: $\frac{\partial \rho}{\partial t} + \nabla \cdot (\rho \vec{v}) = 0$

The Equation of Motion: $\rho \frac{\partial \vec{v}}{\partial t} + \rho(\vec{v} \cdot \nabla) \vec{v} = -\nabla p + \frac{1}{\mu} (\nabla \times \vec{B}) \times \vec{B} + \vec{F}$

The Induction Equation: $\frac{\partial \vec{B}}{\partial t} = \nabla \times (\vec{v} \times \vec{B}) + \eta \nabla^2 \vec{B}$

The Energy Equation: $\frac{\partial p}{\partial t} + \vec{v} \cdot \nabla p + \gamma p \nabla \cdot \vec{v} = 0$

Where Ampere's equation has been used to eliminate \vec{j} from the Lorentz force term in the equation of motion, and non-adiabatic sources of energy have been ignored in the energy equation. The extra force term in the motion equation may include gravity and/or any viscous terms.

These are two vector equations and two scalar equations for a total of 8 equations. The unknowns are \vec{v} , \vec{B} , ρ , and p – two scalar and two vector quantities, for a total of eight quantities. So these equations, together with the appropriate boundary and initial conditions, should be enough to completely determine the relevant solutions to any well-posed physical problem involving the solar atmosphere. Once \vec{v} and \vec{B} are found, Ampere's equation can be used to find \vec{j} and Ohm's law to find \vec{E} .

The initial configuration of a magnetic field is often set up in terms of flux tubes or current sheets. We now examine these structures.

2.6 Flux Tubes and Current Sheets

The basic units used to model structures in the solar atmosphere are flux tubes and current sheets. They are usually considered as isolated entities, but can also be made to interact with each other and the surrounding atmosphere. We review them one at a time.

2.6.1 Flux Tubes

As the name suggests, a flux tube is a three dimensional region filled with a prescribed magnetic field between two non-coplanar simple closed curves. The field lines can be

thought of as filling the region with a magnetic “flow” or flux. The closer the lines the stronger the field, and the further apart the weaker the field. Since $\vec{B} = \langle B_x, B_y, B_z \rangle$ is tangent to the field lines, we can graph them by solving the equations $\frac{dx}{B_x} = \frac{dy}{B_y} = \frac{dz}{B_z}$. The strength of the field at a particular cross-section of the tube can be defined as a flux integral, $\iint_S \vec{B} \cdot d\vec{S}$, where $d\vec{S}$ is taken in the same direction as \vec{B} so that the strength will always be positive.

A nice property of flux tubes is that the strength is the same at all cross-sections. This follows from the following argument (see figure 2.1):

Let S_1 and S_2 be two cross-sections and S be a surface connecting them (along the field lines) to form a volume V , then:

$$\begin{aligned} \iint_{S \cup S_1 \cup S_2} \vec{B} \cdot d\vec{S} &= \iint_S \vec{B} \cdot d\vec{S} + \iint_{S_1} \vec{B} \cdot d\vec{S} + \iint_{S_2} \vec{B} \cdot d\vec{S} \\ &= \iint_{S_1} \vec{B} \cdot d\vec{S} + \iint_{S_2} \vec{B} \cdot d\vec{S} = 0, \end{aligned}$$

since $\iint_{S \cup S_1 \cup S_2} \vec{B} \cdot d\vec{S} = \iiint_V \nabla \cdot \vec{B} dV = 0$ by the divergence theorem (and the solenoidal condition) and $\iint_S \vec{B} \cdot d\vec{S} = 0$ since \vec{B} and $d\vec{S}$ are orthogonal over S . So $\iint_{S_1} \vec{B} \cdot d\vec{S} = -\iint_{S_2} \vec{B} \cdot d\vec{S}$. Take the absolute value and the result follows.

Note that since the strength of the field is the same at any cross-section, it follows that as the tube narrows the mean field must gain strength and as the tube widens the mean field must weaken.

2.6.2 Current Sheets

In most solar applications the magnetic field is spread over a large region. This makes the current density \vec{j} ($\approx \frac{B}{\mu L}$) small. But if two regions of magnetic field (two flux tubes for example) become close, and we want to model the region between them, then we are looking at a smaller length scale and a higher current density. This type of domain is known as a current sheet. It is a non-propagating boundary separating two regions of fluid with its magnetic field squeezed between and tangent to both boundaries. Essentially it is a tangential discontinuity in a larger domain of plasma. Note that due to the smaller length scale $R_m \ll 1$, so diffusion dominates in the current sheet.

A current sheet can be thought of as a stationary shock wave. It separates two regions of fluid where the equations of MHD hold, and its properties are governed by diffusive effects. Standing waves can result from plasma being ejected from the ends of the sheet. The magnetic field forming the sheet can diffuse into the surrounding plasma, converting its magnetic energy into heat (a process known as ohmic diffusion) and plasma motion.

2.7 Magnetohydrostatics

Many solar phenomena remain in equilibrium for long periods of time. The magnetic field is frozen into the fluid and provides a magnetic pressure to balance the sources of fluid pressure. In this static case we can set $\vec{v} \equiv \vec{0}$ and $\frac{\partial}{\partial t} \equiv 0$ so the equation of

motion becomes:

$$-\nabla p + \vec{j} \times \vec{B} + \rho \vec{g} = \vec{0},$$

expressing the magnetohydrostatic balance of forces. In certain situations some of these forces dominate the others. For example, if $\vec{g} = \langle 0, 0, -g \rangle$ and s is an arc-length parameter along the magnetic field lines (so $ds \cos \theta = dz$ where θ is the angle between \vec{B} and the vertical) then the component of the above equation in the direction of \vec{B} is $-\frac{dp}{ds} - \rho g \cos \theta = 0$ (see figure 2.2). This $\Rightarrow -\frac{dp}{dz} - \rho g = 0$ where p and ρ are functions of z alone. Now $p = c \cdot \rho T$ (the equation of state) where c is a constant, so $T = T(z)$ and we obtain the differential equation $\frac{dp}{dz} + \frac{\rho}{c} \frac{p}{T} = 0$. The solution is:

$$p(z) = p_0 \exp\left(-\int_0^z \frac{1}{\Lambda(s)} ds\right),$$

where p_0 is the pressure at $z = 0$ and $\Lambda(s) = \frac{c}{g} T(s)$ is called the pressure scale height. Hence the pressure following a magnetic field line decreases exponentially. If the atmosphere is isothermal then Λ is constant and $p = p_0 e^{-\frac{z}{\Lambda}}$, with Λ being the height over which the pressure falls by a factor of e^{-1} . Hence, if L is a typical length scale for a problem and $L \ll \Lambda$ then gravity can be neglected.

Note that $p_0 = p_0(x, y)$ is the pressure at $z = 0$. If this pressure is constant then the pressure is the same at a fixed height and the atmosphere is plane-parallel. However, if the base pressure changes then this change will propagate up the atmosphere along the field lines at the sound speed.

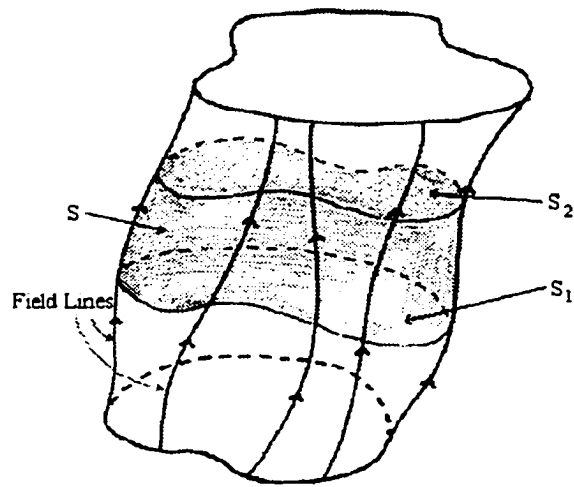


Fig. 2.1: A Flux Tube.

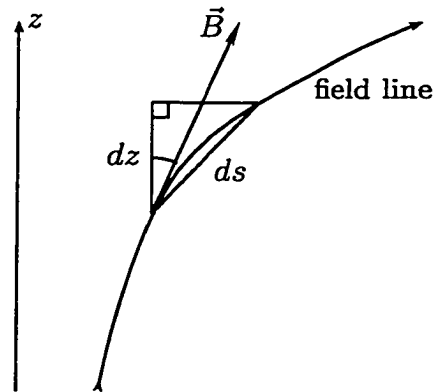


Fig. 2.2: ds and dz on a field line.

2.7.1 The Plasma Beta

Other approximations can be made depending on the relative strengths of the pressure gradient compared to the Lorentz force. The magnitude of the pressure gradient is $\frac{P}{L}$ and that of the magnetic pressure is $\frac{B^2}{\mu L}$ so define a quantity called the plasma beta:

$$\beta = \frac{2P\mu}{B^2} = \frac{\text{gas pressure}}{\text{magnetic pressure}}.$$

If $\beta \gg 1$ then the pressure gradient dominates, while if $\beta \ll 1$ the Lorentz force dominates and (if gravity can be neglected also) we get $\vec{j} \times \vec{B} = \vec{0}$. In this case the magnetic field is called force-free.

2.7.2 Potential Fields

A special case of force-free fields occurs when $\vec{j} \equiv \vec{0}$. Then Ampere's equation becomes $\nabla \times \vec{B} = \vec{0}$ which $\Rightarrow \vec{B} = \nabla\Phi$ for some potential function Φ . So a current-free field is also called a potential field. Taking the divergence of both sides, it follows from the solenoidal condition that Φ is a solution to Laplace's equation $\nabla^2\Phi = 0$. This of course, can be solved by a variety of methods from separation of variables to conformal mapping, depending on the context.

2.7.3 Force-Free Fields

If $L \ll \Lambda$, $\beta \ll 1$ but $\vec{j} \neq \vec{0}$ everywhere, then $\vec{j} \times \vec{B} = \vec{0} \Rightarrow \vec{j}$ and \vec{B} are parallel. Thus, $\mu\vec{j} = \alpha\vec{B}$ which implies, by Ampere's equation that:

$$\nabla \times \vec{B} = \alpha\vec{B} \quad (\text{where } \alpha = \alpha(\vec{x}) \text{ in general}).$$

Taking the divergence of the above we get $\vec{B} \cdot \nabla \alpha = 0$; therefore \vec{B} must be tangent to surfaces of constant α . Even though α is a function of position, it must remain constant along individual field lines.

Note that if α is constant everywhere then taking the curl of both sides, and using the identity $\nabla \times \nabla \times \vec{B} = \nabla(\nabla \cdot \vec{B}) - \nabla^2 \vec{B}$, yields $(\nabla^2 + \alpha^2)\vec{B} = \vec{0}$, a linear Helmholtz equation, while if α varies across field lines then a nonlinear coupled system, $\nabla^2 \vec{B} + \alpha^2 \vec{B} = \vec{B} \times \nabla \alpha$ with $\vec{B} \cdot \nabla \alpha = 0$ results.

2.7.4 MagnetoStatics and Flux Tubes

A useful special case of static equilibrium is the cylindrically symmetric flux tube with $\vec{B} = \langle 0, B_\theta(r), B_z(r) \rangle$. The field lines are found by solving $\frac{r d\theta}{B_\theta} = \frac{dz}{B_z}$, so they are helices twisting around the cylinder with radius r . If we suppose that the flux tube has length $2L$ then a particular field line has a total twist of:

$$\Phi(r) = \int d\theta = \int_0^{2L} \frac{B_\theta}{r B_z} dz = \frac{2L B_\theta}{r B_z}.$$

This quantity is called the twist of the flux tube. Neglecting gravity, the force balance equation in cylindrical coordinates is $\frac{dp}{dr} + \frac{d}{dr} \left(\frac{B_\theta^2 + B_z^2}{2\mu} \right) + \frac{B_\theta^2}{\mu r} = 0$. Any two of the three dependent variables can be fixed and the third one obtained. Note that if B_θ and B_z are prescribed, this is equivalent to fixing the twist of the flux tube. If $B_\theta \equiv 0$ (the axial case) then the equation simply says that the total pressure (plasma and magnetic) is constant.

2.8 Waves

An important method of distributing matter and energy in a plasma is by means of waves. Even if the wave amplitude is small (so there is no bulk motion of plasma) energy can still be transported. If the wave amplitude is large then shock waves can form, and these have important consequences for the properties of the fluid. All waves transport energy from a source throughout the plasma and are supported by restoring forces. In the solar atmosphere there are three basic restoring forces that produce different wave modes. The fluid pressure acts to produce sound waves. The magnetic tension produces a wave unique to MHD called Alfvén waves, and buoyancy gives rise to internal gravity waves (the word internal is used here to distinguish such waves from surface waves between two fluids). There is a fourth type of wave mode called inertial waves that result from solar rotation (Coriolis forces), but these modes will not be considered here. The energy transported by rotation is significantly less than that of the other modes.

To determine which wave modes propagate and which decay the fluid is first assumed to be in a state of equilibrium, and then a perturbation is added that is much smaller than this basic state. This is substituted into the governing equations and they can then be simplified using the equilibrium solution. The equations are then linearised by neglecting any products of the small perturbation terms. Once we have linear equations, a plane wave solution can be assumed which will lead to a dispersion relation. This is a relationship between the wavelength and the frequency that can determine which modes can propagate.

The basic equations are (neglecting any dissipative forces like viscosity, and assuming frozen field lines):

$$\begin{aligned}\frac{\partial \rho}{\partial t} + \nabla \cdot (\rho \vec{v}) &= 0 \\ \rho \frac{\partial \vec{v}}{\partial t} + \rho (\vec{v} \cdot \nabla) \vec{v} &= -\nabla p + \frac{1}{\mu} (\nabla \times \vec{B}) \times \vec{B} + \rho \vec{g} \\ \frac{\partial \vec{B}}{\partial t} &= \nabla \times (\vec{v} \times \vec{B}) \\ \frac{\partial p}{\partial t} + \vec{v} \cdot \nabla p + \gamma p \nabla \cdot \vec{v} &= 0.\end{aligned}$$

Now, let

$$\begin{aligned}\vec{B} &= \vec{B}_0 + \vec{B}_1 \\ \vec{v} &= \vec{0} + \vec{v}_1 \\ \rho &= \rho_0 + \rho_1 \\ p &= p_0 + p_1,\end{aligned}$$

where the “0” subscripts satisfy the equilibrium equations (i.e. $\nabla p_0 = \frac{1}{\mu} (\nabla \times \vec{B}_0) \times \vec{B}_0 + \rho_0 \vec{g}$ and $\nabla \cdot \vec{B}_0 = 0$) and the “1” subscripts are small in comparison to the “0” subscripts (i.e. $|\rho_1| \ll |\rho_0|$, etc.) and are functions of space and time. Substitute these into the basic equations above, simplify and linearise to get:

$$\begin{aligned}\frac{\partial \rho_1}{\partial t} + \nabla \cdot (\rho_0 \vec{v}_1) &= 0 \\ \rho_0 \frac{\partial \vec{v}_1}{\partial t} &= -\nabla p_1 + \frac{1}{\mu} (\nabla \times \vec{B}_1) \times \vec{B}_0 + \frac{1}{\mu} (\nabla \times \vec{B}_0) \times \vec{B}_1 + \rho_1 \vec{g} \\ \frac{\partial \vec{B}_1}{\partial t} &= \nabla \times (\vec{v}_1 \times \vec{B}_0) \\ \frac{\partial p_1}{\partial t} + \vec{v}_1 \cdot \nabla p_0 + \gamma p_0 \nabla \cdot \vec{v}_1 &= 0.\end{aligned}$$

These equations can be reduced to one equation by taking $\frac{\partial}{\partial t}$ of the motion equation, then using the others to eliminate ρ_1 , p_1 and \vec{B}_1 :

$$\begin{aligned}\rho_0 \frac{\partial^2 \vec{v}_1}{\partial t^2} &= \nabla (\vec{v}_1 \cdot \nabla p_0 + \gamma p_0 \nabla \cdot \vec{v}_1) + \frac{1}{\mu} \left(\nabla \times \nabla \times (\vec{v}_1 \times \vec{B}_0) \right) \times \vec{B}_0 \\ &\quad + \frac{1}{\mu} (\nabla \times \vec{B}_0) \times \nabla \times (\vec{v}_1 \times \vec{B}_0) - \nabla \cdot (\rho_0 \vec{v}_1) \vec{g}.\end{aligned}\tag{2.1}$$

This is the linearised equation of motion and describes the evolution of all linear MHD waves [7]. To provide physical insight we first simplify this equation to obtain each pure wave mode alone.

2.8.1 Sound Waves

Setting $\vec{B}_0 = \vec{g} = \vec{0}$ ensures that the only restoring force is fluid pressure. Here $\beta = \infty$ and $L \ll \Lambda$. This will isolate the acoustic modes. Since the equilibrium pressure satisfies $\nabla \cdot p_0 = 0$, p_0 is constant and the linearised equation of motion (2.1) becomes $\rho_0 \frac{\partial^2 \vec{v}_1}{\partial t^2} = \nabla(\gamma p_0 \nabla \cdot \vec{v}_1)$. Now assume constant density and take the divergence of both sides to get $\frac{\partial^2}{\partial t^2}(\nabla \cdot \vec{v}_1) = \frac{\gamma p_0}{\rho_0} \nabla^2(\nabla \cdot \vec{v}_1)$. Setting $\Psi = \nabla \cdot \vec{v}_1$ gives a wave equation in the divergence of the velocity perturbation (i.e. compressibility is propagated):

$$\frac{\partial^2 \Psi}{\partial t^2} = c_s^2 \nabla^2 \Psi \quad \text{where} \quad c_s^2 = \frac{\gamma p_0}{\rho_0} \quad (\text{the square of the sound speed}).$$

Note that a non-zero Ψ implies that sound waves only propagate in a compressible medium. This wave equation has constant coefficients so we assume the standard plane wave solution $\Psi = \hat{\Psi} e^{i(\vec{k} \cdot \vec{r} - \omega t)}$ where:

$\hat{\Psi} = \text{a constant}$

$\vec{k} = \text{a wave vector that points in the direction of propagation}$

$\vec{r} = \langle x, y, z \rangle = \text{a position vector}$

$\omega = \text{a (possibly complex) frequency.}$

Substituting in this solution gives $\omega^2 = c_s^2 \|\vec{k}\|^2$ giving the dispersion relation (letting $k = \|\vec{k}\|$):

$$\omega = \pm c_s k.$$

The dispersion relation can be used to define two important quantities, the phase velocity and the group velocity. The phase velocity $\vec{v}_p = \frac{\omega}{k} \hat{k}$, where \hat{k} is the unit vector in the direction of \vec{k} , gives the velocity of a single wave. Note that if ω is not proportional to k then waves of different wave numbers travel at different speeds and the wave propagation is said to be dispersive. Any initial condition composed of a variety of Fourier components will tend to spread out as the wave progresses. The group velocity is defined as $\vec{v}_g = \nabla_{\vec{k}} \omega = \left\langle \frac{\partial \omega}{\partial k_1}, \frac{\partial \omega}{\partial k_2}, \frac{\partial \omega}{\partial k_3} \right\rangle$ and gives the velocity of the envelope for a wave packet. A group of waves transports energy at this velocity. If ω is proportional to k then the group velocity will be constant and $\vec{v}_p = \vec{v}_g$. For sound waves $\vec{v}_p = \vec{v}_g = \pm c_s \hat{k}$, so sound waves propagate isotropically.

2.8.2 Alfvén Waves

Next we isolate the effect of the Lorentz force. Let $p_0 = 0$ and $\vec{g} = \vec{0}$, so $L \ll \Lambda$ and the plasma is low beta ($\beta = 0$). Furthermore, let the equilibrium magnetic field be uniform. The linearised equation of motion (2.1) then reduces to:

$$\rho_0 \frac{\partial^2 \vec{v}_1}{\partial t^2} = \frac{1}{\mu} \left(\nabla \times \nabla \times (\vec{v}_1 \times \vec{B}_0) \right) \times \vec{B}_0.$$

Now assume a plane wave solution for \vec{v}_1 , namely $\vec{v}_1 = \vec{v} e^{i(\vec{k} \cdot \vec{r} - \omega t)}$ where \vec{v} is a constant vector, (note that with this solution form $\nabla \times = -i\vec{k} \times$) to get $\frac{\mu \rho_0 \omega^2}{B_0^2} \vec{v} = \left(\vec{k} \times \vec{k} \times (\vec{v} \times \hat{B}_0) \right) \times \hat{B}_0$, where $B_0 = \|\vec{B}_0\|$ and \hat{B}_0 is a unit vector in the direc-

tion of \vec{B}_0 . Using the vector identities $\vec{A} \times (\vec{B} \times \vec{C}) = (\vec{A} \cdot \vec{C})\vec{B} - (\vec{A} \cdot \vec{B})\vec{C}$ and $(\vec{A} \times \vec{B}) \times \vec{C} = (\vec{A} \cdot \vec{C})\vec{B} - (\vec{B} \cdot \vec{C})\vec{A}$ and letting $c_a = \frac{B_0}{\sqrt{\mu\rho_0}}$, the following equation is found:

$$\frac{\omega^2}{c_a^2} \vec{v} = k^2 \cos^2 \theta \vec{v} - (\vec{k} \cdot \vec{v})k \cos \theta \hat{B}_0 + [(\vec{k} \cdot \vec{v}) - (\hat{B}_0 \cdot \vec{v})k \cos \theta] \vec{k},$$

where θ is the angle between the direction of propagation (\vec{k}) and the constant equilibrium field (\vec{B}_0). This equation can be simplified by taking the dot product of both sides with \hat{B}_0 . The first and last terms cancel, together with the two middle terms, to show that $\vec{v} \cdot \hat{B}_0 = 0$. The last term can now be neglected. Now take the dot product with \vec{k} (cancelling the first two terms) to get:

$$(\omega^2 - c_a^2 k^2)(\vec{k} \cdot \vec{v}) = 0.$$

This equation has two solutions. Either $\vec{k} \cdot \vec{v} = 0$ or $\omega = \pm c_a k$. If $\vec{k} \cdot \vec{v} = 0$ then we get the dispersion relation:

$$\omega = \pm c_a k \cos \theta.$$

This gives both a phase and group velocity of:

$$\vec{v}_p = \vec{v}_g = \pm c_a \cos \theta \hat{k}.$$

This means that wave fronts in the direction of the magnetic field propagate (and carry energy) at the speed c_a along the field lines. The field lines act as taut strings carrying transverse waves (since \vec{k} and \vec{v} are orthogonal). These waves are called Alfvén waves and c_a is known as the Alfvén speed. If the direction of propagation is normal to the field lines then there is no wave motion. The fluid simply carries the

field lines with it. These types of waves are called shear Alfvén waves (or “slow-mode” waves if the gas pressure is included but dominates the magnetic pressure) and are due to the magnetic tension in the field lines.

The other solution, $\omega = \pm c_a k$, gives a phase and group velocity of:

$$\vec{v}_p = \vec{v}_g = \pm c_a \hat{k}.$$

These waves do not depend on the direction of the field and propagate isotropically with speed c_a . These are known as compressional Alfvén waves (or “fast-mode” waves if the gas pressure is included but is dominated by the magnetic pressure) and are due to the magnetic pressure (see figure 2.3). Note that if $\theta = \frac{\pi}{2}$ then the field lines carry waves longitudinally, much as sound waves are propagated.

2.8.3 Gravity Waves

We now ignore the magnetic field and include gravity. For simplicity we assume that the density and pressure of the fluid are vertically stratified, increasing with depth, and that gravity acts vertically ($\vec{g} = -g\hat{z}$). This density stratification leads to buoyancy forces that produce waves called gravity waves. If the density of a fluid element does not match that of its surroundings then it will either rise or fall. If such an element is initially in equilibrium with its surroundings at the equilibrium density and pressure of ρ_0 and p_0 respectively (see figure 2.4), for the element to be in equilibrium the equation of hydrostatic equilibrium $\frac{dp_0}{dz} = -\rho_0 g$ must be satisfied throughout. Now say the element is displaced by a small height dz , with the following assumptions:

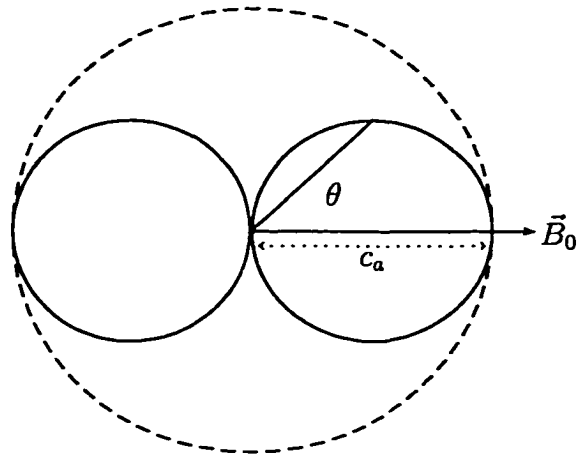


Fig. 2.3: A polar diagram for shear (solid) and compressional (dashed) Alfvén waves.

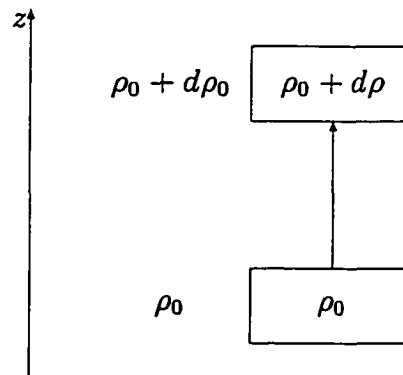


Fig. 2.4: A rising parcel of fluid.

i) the motion is slow enough that the element remains in pressure equilibrium with the surrounding fluid (this is necessary if we want to ignore sound waves) and

ii) the motion is fast enough to be adiabatic (i.e. no heat is lost or gained by the element).

If ρ and p are the density and pressure in the element after displacement, then assumption ii) $\Rightarrow \frac{p}{\rho^\gamma}$ is constant. So $dp = \frac{\gamma p}{\rho} d\rho = c_s^2 d\rho$. Therefore, using assumption i), $d\rho = -\frac{\rho_0 g}{c_s^2} dz$. The buoyancy force is $g(d\rho_0 - d\rho)$, so if $d\rho < d\rho_0$ the element will rise and if $d\rho > d\rho_0$ then the element will fall. Now, using $d\rho_0 = \frac{d\rho_0}{dz} dz$ we find that the buoyant force is:

$$g \left[\frac{1}{\rho_0} \frac{d\rho_0}{dz} + \frac{g}{c_s^2} \right] \rho_0 dz = -N^2 \rho_0 dz$$

where $N^2 = -g \left[\frac{1}{\rho_0} \frac{d\rho_0}{dz} + \frac{g}{c_s^2} \right]$ is called the Brunt-Väisälä frequency. To see why this quantity is called a frequency, write the equation of motion for the element: $\rho_0 \frac{d^2(dz)}{dt^2} = -N^2 \rho_0 dz$. The element will move in simple harmonic motion with angular frequency N as long as $N^2 > 0$.

To derive a dispersion relation for gravity waves, start with the linearized equation of motion (2.1) with \vec{B}_0 set to zero, vertically stratify the density by letting $\rho_0 = \rho_0(z) = \text{constant} \cdot e^{-\frac{z}{\Lambda}}$ where Λ is the scale height, and let $\vec{v}_1 = \vec{v} e^{i(\vec{k} \cdot \vec{r} - \omega t)}$. This will lead to:

$$\omega^2 \vec{v} = c_s^2 (\vec{k} \cdot \vec{v}) \vec{k} + i g \tilde{v}_z \vec{k} + i(\gamma - 1) g (\vec{k} \cdot \vec{v}) \hat{z},$$

where \tilde{v}_z is the z component of \vec{v} and \hat{z} is the standard unit vector directed vertically upwards. Next take the dot product of both sides of this equation with \vec{k} , then with

\hat{z} , and eliminate the $\frac{\vec{k} \cdot \vec{v}}{\hat{v}_z}$ term between the resulting system to get:

$$\omega^4 - (i\gamma g k_z + c_s^2 k^2)\omega^2 + (\gamma - 1)g^2(k^2 - k_z^2) = 0. \quad (2.2)$$

At this point we can take advantage of the fact that we are neglecting sound waves that would swamp any waves caused by buoyancy, so $\omega \ll kc_s$. This is known as the Boussinesq approximation – the fluid is considered as incompressible, but variations in density are still included in the buoyancy term so this force alone drives any fluid motions. With this in mind, the above dispersion relation becomes $k^2\omega^2c_s^2 = (\gamma - 1)g^2(k^2 - k_z^2)$. Now using the exponential form for the density stratification (valid in an isothermal medium), the Brunt-Väisälä frequency can be written as $N^2 = -g \left[\frac{1}{\rho_0} \frac{d\rho_0}{dz} + \frac{g}{c_s^2} \right] = \frac{(\gamma-1)g^2}{c_s^2}$. The above dispersion relation can then be written as:

$$\omega = \pm N \sin \theta.$$

where θ is the angle between \vec{k} and \hat{z} . Note that $\omega \leq N$ so gravity waves cannot propagate faster than the Brunt-Väisälä frequency, and that they do not move vertically. Also note that the z component of the group velocity is $\frac{\partial \omega}{\partial k_z} = -\frac{k_z}{k^2}\omega$, so energy flows down when waves propagate up.

2.8.4 Magnetoacoustic Waves

We now consider combinations of two of the basic three restoring forces. If the magnetic and fluid pressure are comparable, but $L \ll \Lambda$ (so we can neglect gravity), we will combine the properties of the magnetic and sound waves. The compressibility of the plasma and the magnetic field will interact. The linearized equation of motion

(2.1) will be:

$$\rho_0 \frac{\partial^2 \vec{v}_1}{\partial t^2} = \nabla(\vec{v}_1 \cdot \nabla p_0 + \gamma p_0 \nabla \cdot \vec{v}_1) + \frac{1}{\mu} \left(\nabla \times \nabla \times (\vec{v}_1 \times \vec{B}_0) \right) \times \vec{B}_0 + \frac{1}{\mu} (\nabla \times \vec{B}_0) \times \nabla \times (\vec{v}_1 \times \vec{B}_0).$$

Assuming the equilibrium field to be constant, setting $\vec{v}_1 = \vec{v} e^{i(\vec{k} \cdot \vec{r} - \omega t)}$ and simplifying as above, this becomes:

$$\frac{\omega^2}{c_a^2} \vec{v} = k^2 \cos^2 \theta \vec{v} - (\vec{k} \cdot \vec{v}) k \cos \theta \hat{B}_0 + \left[\left(1 + \frac{c_s^2}{c_a^2} \right) (\vec{k} \cdot \vec{v}) - (\hat{B}_0 \cdot \vec{v}) k \cos \theta \right] \vec{k},$$

where θ is again the angle between \vec{k} and \vec{B}_0 . Now take the dot product of this equation with \vec{k} , then \hat{B}_0 , and eliminate $\frac{\vec{k} \cdot \vec{v}}{\hat{B}_0 \cdot \vec{v}}$ from the resulting system, to get the dispersion relation for magnetoacoustic waves:

$$\omega^4 - k^2 (c_s^2 + c_a^2) \omega^2 + c_s^2 c_a^2 k^4 \cos^2 \theta = 0.$$

Using the quadratic formula we get:

$$\vec{v}_p = \frac{\omega}{k} \hat{k} = \pm \frac{1}{\sqrt{2}} \left[c_s^2 + c_a^2 \pm \sqrt{c_s^4 + c_a^4 - 2c_s^2 c_a^2 \cos 2\theta} \right]^{\frac{1}{2}} \hat{k}.$$

A polar plot shows the two distinct phase speeds quite well. There is clearly a fast (almost isotropic) wave and a slow wave (see figure 2.5).

2.8.5 Acoustic-Gravity Waves

The dispersion relation for compressible and buoyant forces will be the same as initially obtained for gravity waves (2.2), but we cannot simplify the equation by neglecting compressibility. By introducing an extra parameter $N_s = \frac{\gamma g}{2c_s}$ and introducing another wave vector \vec{k}' as $\vec{k}' = \vec{k} + i \frac{\gamma g}{2c_s^2} \hat{z}$ we can rewrite the relation as:

$$\omega^4 - (N_s^2 + k'^2 c_s^2) \omega^2 + N^2 k'^2 c_s^2 \sin^2 \theta' = 0,$$

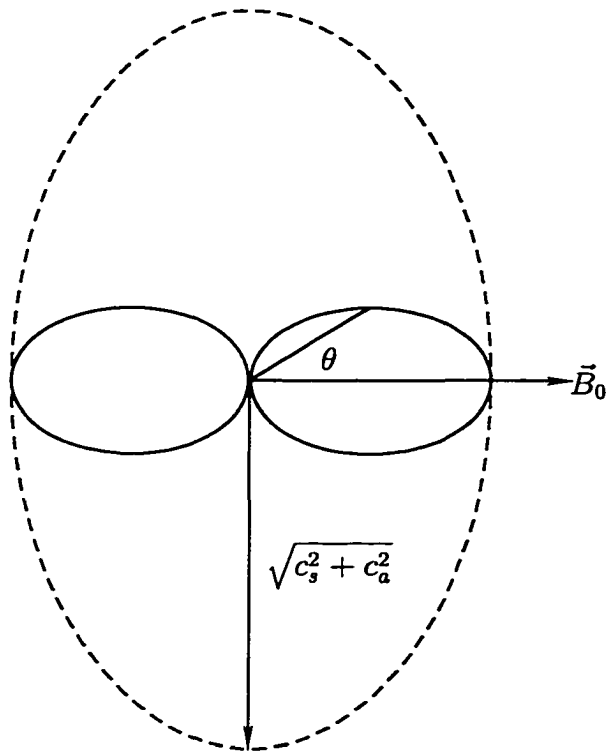


Fig. 2.5: Polar diagram for fast (dashed) and slow (solid) magnetoacoustic waves. The semi-major axis of the smaller ellipse is the smaller of c_s and c_a .

where θ' is the angle between \vec{k}' and \hat{z} . The introduction of the wave vector \vec{k}' changes the velocity perturbation to $\vec{v} = \bar{v} e^{\frac{\lambda g z}{2c_s^2}} e^{i(\vec{k}' \cdot \vec{r} - \omega t)}$, so waves can grow exponentially.

To see which modes propagate for a given horizontal wave number $k'_x (= k_x)$ we can let $k'^2 = k_z'^2 + k_x^2$ to get:

$$\omega^4 - (N_s^2 + k_x^2 c_s^2) \omega^2 + N^2 k_x^2 c_s^2 = k_x^2 c_s^2 \omega^2,$$

and then note that disturbances will propagate vertically when the left hand side is positive. This gives the $\omega - k_x$ diagnostic diagram (see figure 2.6).

Unlike the magnetoacoustic waves, these modes are only weakly coupled – the high-frequency modes remain acoustic in nature and the low-frequency modes propagate as gravity waves. The waves with frequencies between N and N_s are evanescent.

2.8.6 Magnetoacoustic-Gravity Waves

Adding a magnetic field to the acoustic-gravity case (or gravity to the magnetoacoustic case) adds another restoring force and another preferred direction. All the terms in the linearized equation of motion (2.1) have to be included, complicating the situation. The waves supported by all three restoring forces – compressibility, gravity and the Lorentz force – are often referred to as magneto-atmospheric waves. Applications to the Solar atmosphere include waves in sunspots [8], waves induced in the corona by sudden events such as flares [9] and heating of the corona [10] (although a more recent explanation is resonant absorption of Alfvén waves in coronal loops [11]). For a detailed treatment of such waves see [12]. Various special cases (boundary conditions, horizontal magnetic fields etc.) lead to many methods used in applied mathematics,

from transform theory to WKB approximation methods [9, 13].

2.9 MHD Instabilities

In MHD, as in ordinary fluid dynamics, stability theory can be applied to determine what values of certain variables or parameters in a particular fluid configuration will cause that configuration to develop nonlinearities and ultimately turbulence. The underlying idea is similar to the plane wave analysis used to determine the wave modes that propagate in a plasma. First a basic flow is established that satisfies the equations and any boundary conditions. This basic flow is modified by adding small perturbation terms and then substituting into the governing equations. These equations are then simplified using the fact that the basic flow satisfies them and linearized by neglecting any products of the small perturbations. Now that the equations are linear, any disturbance can be treated as a superposition of individual modes that can be treated separately. Each mode $f(\vec{x}, t; \omega)$ is then assumed to be of the form $g(\vec{x})e^{\omega t}$, where ω is complex. Substituting this form into the linearized equations gives an eigenvalue/eigenfunction problem. The nature of the eigenvalues, ω then determines the stability of the system. If ω^2 is real and negative for all ω (at all points \vec{x}), for example, then the configuration is stable. The system will simply oscillate about the basic flow. If, however, for at least one mode ω^2 is real and positive then that mode will grow exponentially and dominate the system. The flow is then said to be unstable.

Any basic flow studied in fluid mechanics can be analyzed in MHD by (in principle)

adding a magnetic field. Since a magnetic field has the effect of adding rigidity to a plasma, an otherwise unstable configuration may become stable. Consider for example, the case of Kelvin-Helmholtz instability. Here two incompressible, inviscid fluids flow in parallel horizontal streams at constant velocity u_1 and u_2 ($u_1 \neq u_2$). If the density of the upper fluid is ρ_1 and the lower fluid ρ_2 (with $\rho_1 < \rho_2$) then it can be shown that the interface is unstable to disturbances with wavenumber $k > \frac{g(\rho_2^2 - \rho_1^2)}{\rho_1 \rho_2 (u_1 - u_2)^2}$ [14]. So regardless of the relative speed of the two fluids, small enough wavelengths will be unstable. However if uniform magnetic fields are introduced in each fluid parallel to u_1 and u_2 , then the magnetic tension produces a restoring force stabilizing the interface provided that $B_1^2 + B_2^2 \geq \frac{\mu \rho_1 \rho_2 (u_1 - u_2)^2}{\rho_1 + \rho_2}$ [15].

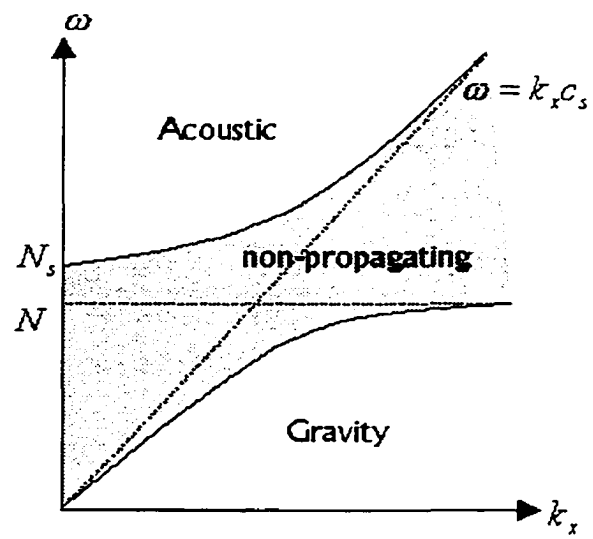


Fig. 2.6: $\omega - k_x$ diagnostic diagram.

CHAPTER 3

A HISTORY OF PROMINENCE MODELS AND MAGNETOCONVECTION

3.1 A History of Prominence Models

A quiescent prominence is a large mass of radiating plasma suspended in the Sun's corona by magnetic fields. First observed during solar eclipses in the 13th century they were thought to be "burning holes in the corona." Later observers described them as "clouds in the lunar atmosphere" or "mountains on the Sun." [16] It was not until the 19th century that they were more exactly described as solar cloud formations. A better understanding of the phenomenon was obtained with the invention of the spectroheliograph (a device that can take a photograph of the Sun at a fixed wavelength) and the coronagraph (a device that uses lenses and an occulting disk to block out the main body of the Sun so the corona can be imaged). Spectroscopy showed that prominences consisted of excited gas hot enough to show emission lines (in fact the element helium was first discovered as an emission line from solar prominence material). The lines were so bright that solar eclipses were no longer necessary to study prominences. The coronagraph allowed photographs of the corona to be taken at any time. In the 1960's the Zeeman and Hanle effects (quantum effects that split and broaden emission lines or enable the polarization of emitted photons to be

measured respectively) enabled the measurement of the strength of the magnetic field in and around prominence material [17].

Quiescent prominences are large, dense and comparatively cool vertical sheets of plasma (see figures 3.1 and 3.2). They are usually referred to as filaments when seen in absorption against the surface of the Sun and prominences when viewed in emission on the limb. They average 200 000 km in length, 50 000 km in height and 6000 km wide – but each of these dimensions can vary by a factor of 10. They are 100–1000 times as dense as their surroundings with an average temperature of 7000 K, cool compared to the surrounding 1 000 000 K corona [5]. Their temperature and density decrease with height. Remarkably stable objects, they remain for days to months arching through the atmosphere. They tend to migrate to the closest pole and are stretched by differential rotation as they travel, although the height and width tend to remain constant [18]. Approximately every 30 000 km, large tree trunk like feet drop into the chromosphere at supergranule boundaries [5]. A low density region called a coronal cavity often surrounds the prominence and an arch of coronal material topped by a “helmet streamer” sits on top of this cavity (see figure 3.3).

At the end of their life, prominences disperse by either slowly breaking up with some material dropping to the surface (usually through the feet) and some escaping into space, or in a sudden explosive event, lasting only hours, where most of its material is ejected into the solar wind. This is known as a coronal mass ejection (see figure 3.4). Resonant absorption of Alfvén waves has been proposed as an explanation for these sudden disappearances [19].

Even though the prominence is threaded by fine ribbons of plasma that move



Fig. 3.1: A prominence seen on the limb of the Sun.

courtesy of the Big Bear Solar Observatory/NJIT

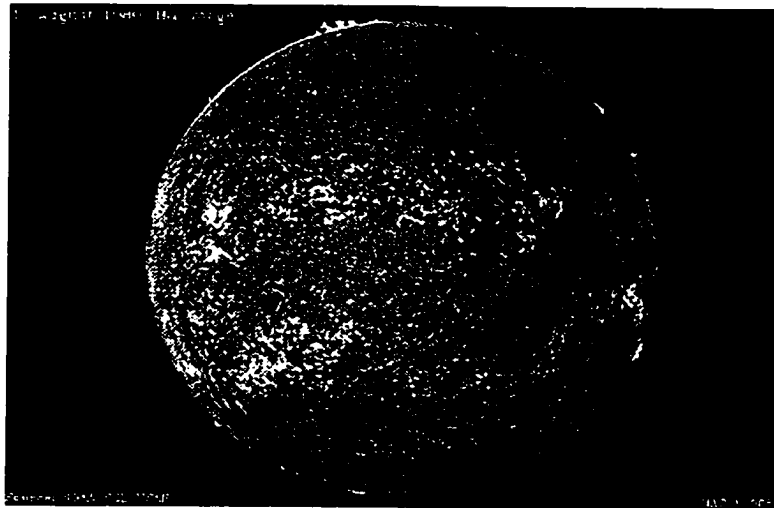


Fig. 3.2: Filaments seen against the surface of the Sun.

courtesy of the High Altitude Observatory/NCAR

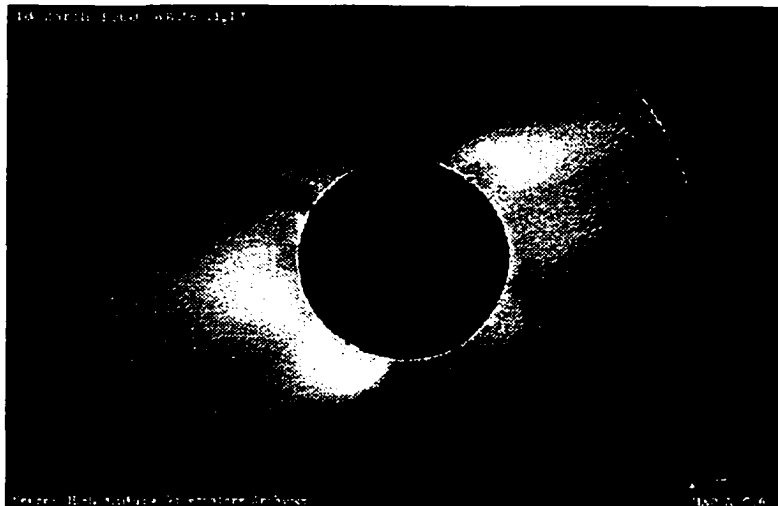


Fig. 3.3: An eclipse photograph showing helmet streamers and coronal cavities above solar prominences.

courtesy of the High Altitude Observatory/NCAR

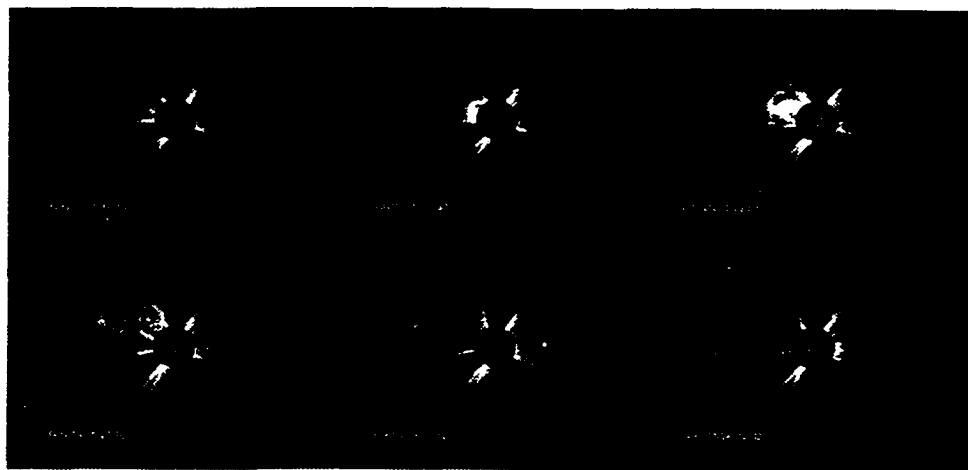


Fig. 3.4: A sequence of photographs showing a coronal mass ejection.

courtesy SOHO/EIT consortium, a project of NASA and ESA

at about 5–15 km/s downward, most models consider them as isothermal blocks of plasma insulated and supported by a magnetic field that is ejected by the convection zone [20]. The field lines are in planes orthogonal to the sheet and the prominence is suspended over a magnetic inversion line, a line with opposite magnetic polarities on either side (see figure 3.5) [21, 22]. Plasma is thought to be supplied to the sheet by either condensation from the corona or injection from the photosphere [18]. Mathematical models are usually divided into two classes; ones that ignore the magnetic field and concentrate on the internal structure of the prominence sheet itself and ones that attempt to model the types of magnetic fields that can support plasma against gravity. Here we are interested in the second type of modeling.

There are two basic recognized types of magnetic topologies that can support plasma in the corona (see figure 3.6). The simplest type are magnetic arcade models of which the prototype is the Kippenhahn-Schlüter model [23]. This is known as a normal polarity model since the field lines above and below the prominence sheet are in the same direction. A more realistic model is the current sheet model called the Kuperus-Raadu model [24]. This model is called inverse polarity since the field lines above and below go in opposite directions. Each of these models will be discussed in detail later, but first we will briefly describe two of the first models developed; those by Menzel [25] and Dungey [26].

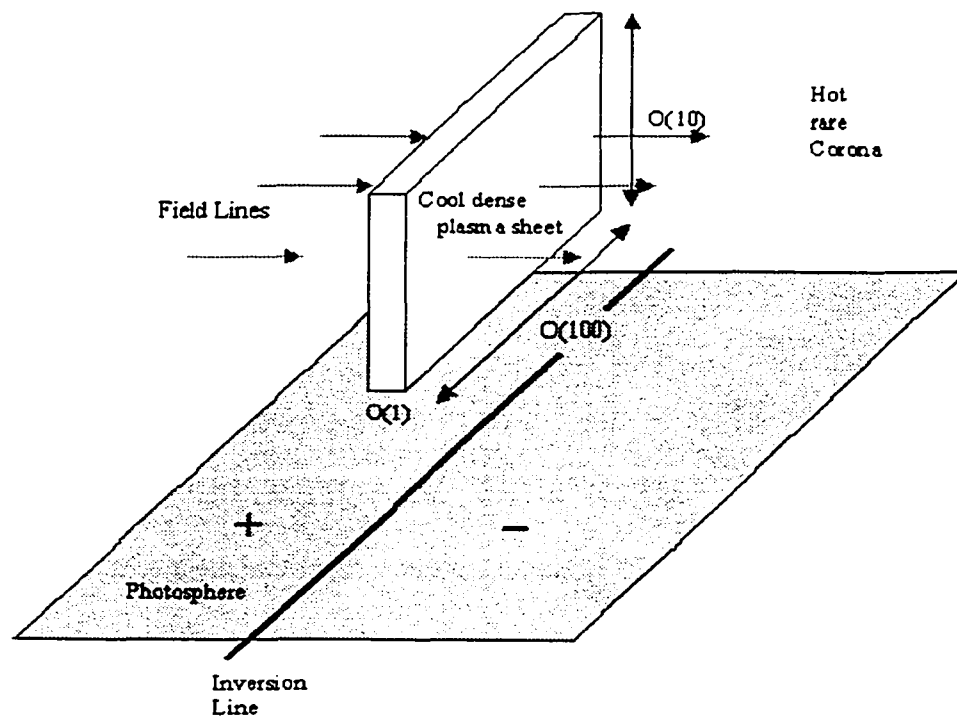


Fig. 3.5: A representative plasma sheet suspended above the photosphere.

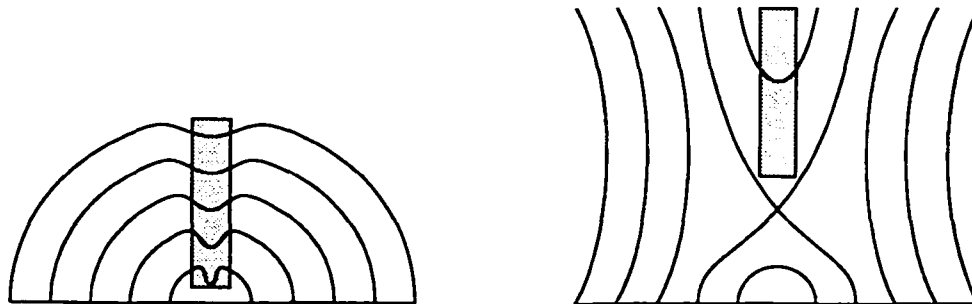


Fig. 3.6: Typical field lines of the KS (left) and KR (right) models, anchored to the photosphere. The base of the figures (x -axis) is the photosphere and the shaded rectangle is a cross-section of the vertical plasma sheet.

3.1.1 The Early Models of Menzel and Dungey

In the early 1950's the detailed photographs of prominences obtained by the coronagraph showed lines of force strung throughout. That, combined with the fact that they tend to form initially in active regions close to sunspots – regions known to have intense magnetic fields, made it clear that magnetism must play a role in the formation of prominences. It was hypothesized that the Lorentz force ($\vec{j} \times \vec{B}$) could support the plasma against gravity and the pressure gradient. Since quiescent prominences appear in static equilibrium for a long period, Menzel, in 1951 [25], looked for the magnetic field to be a solution to the force balance equation $-\nabla p + \vec{j} \times \vec{B} + \rho \vec{g} = \vec{0}$. He assumed that the gas was isothermal (hence the scale height (H) would be a constant and the density could be found from the pressure by the ideal gas law $p = \rho RT$) and that \vec{B} was dependent on the Cartesian variables x and z only, the x -axis orthogonal to the sheet and the y -axis aligned with the prominence axis. He further assumed a flux function $F(x, z)$ for \vec{B} so that $\vec{B} = \langle -\frac{\partial F}{\partial z}, 0, \frac{\partial F}{\partial x} \rangle$ (a contour map of F will then give the field lines) and that $p(x, z)$ along with $F(x, z)$ were separable functions of the form $p = p(x)e^{-\frac{z}{H}}$ and $F = F(x)e^{-\frac{z}{H}}$. These forms gave an ODE for $p(x)$ that could be solved exactly and one for $F(x)$ that had to be solved numerically, but from this equation it could be inferred that the lines of force were periodic in nature. A dip at $x = 0$ could hold plasma with the bulk of the gas being held between two points of inflection [27] (see figure 3.7).

In 1953 Dungey [26] solved the same equation with the same assumption about the pressure variation but made no assumptions about $F(x, z)$. He solved the resulting

PDE using conformal mapping techniques. The solution obtained was $F(x, z) = e^{-\frac{x}{H}} - 2e^{-\frac{x}{2H}} \cos \frac{x}{2H} + 1$ which are closed loops for $F < 1$ and infinite waves for $F > 1$ (see figure 3.8).

Both these models were criticized for their lack of physical reality. Menzel's model predicted prominences to be as wide as they are high [28], and Cowling showed that Dungey's model required currents to flow inside the prominence in opposite directions [20], facts not supported by observation. These models were a good start but a more realistic model was developed in 1957 by Kippenhahn and Schlüter [23].

3.1.2 The Kippenhahn-Schlüter Model

Kippenhahn and Schlüter also solved the force balance equation in equilibrium and assumed the plasma sheet was isothermal but made the assumption that the x component of \vec{B} was a constant, B_x . They further set all dependent variables (p , ρ and B – the z component of \vec{B}) to be functions of x alone. These assumptions gave a simple ODE in B which together with the boundary conditions $B \rightarrow \pm B_z$ (a constant) as $z \rightarrow \pm\infty$ and $B(0) = 0$ yielded the solution $B(x) = B_z \tanh \frac{B_x x}{B_x H}$ which integrates to a flux function of $F(x) = -B_x H \ln(\cosh \frac{B_x x}{B_x H})$ (see figure 3.9).

This model gave more realistic numbers for the pressure and density distribution inside the prominence, so it was widely accepted and used as a basis for many other papers in prominence theory. A major drawback of the model is its assumption that all variables are functions of x alone, so the solution is only valid in a thin region about the prominence. Even though the field lines have the dips needed for plasma

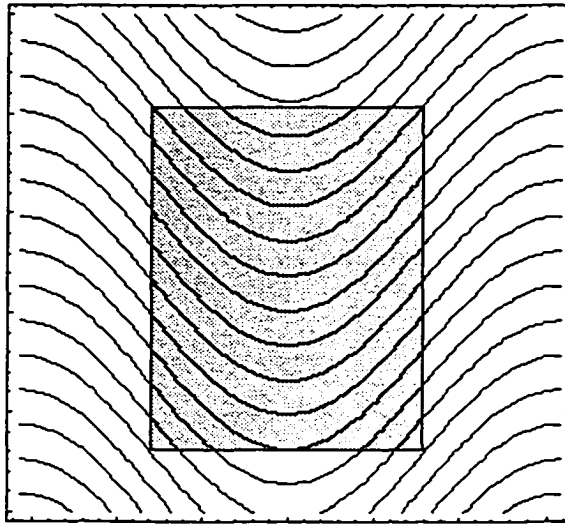


Fig. 3.7: Field lines of Menzel's model. A cross-section of the plasma sheet is shown around the relative minimum of the field lines.

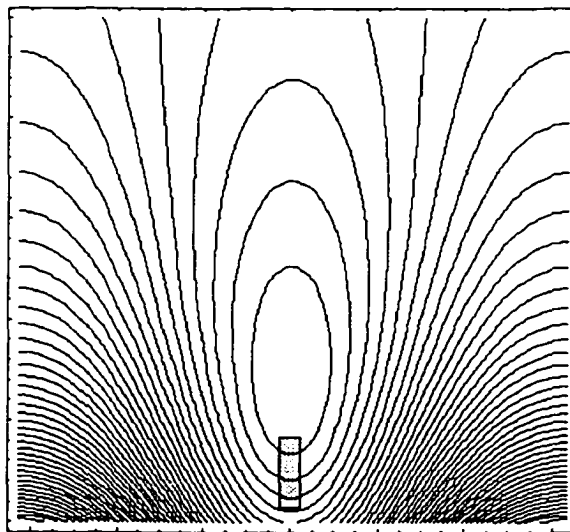


Fig. 3.8: Field lines of Dungey's model.

to collect [29], there is no mechanism connecting the field to the photosphere.

As an interesting mathematical aside, the models of Menzel, Dungey and Kippenhahn-Schlüter were all connected by Brown in 1958 [30, 20]. As with all the above models, Brown assumed the y component of \vec{B} to be zero, and introduced a flux function F for the other components and all dependent variables to be independent of y . The force balance equation could then be rewritten as $\nabla \left(p e^{\frac{z}{H}} \right) = - \left(\nabla^2 F e^{\frac{z}{H}} \right) \nabla F$. This shows that $p e^{\frac{z}{H}}$ is a function of F , say $\Phi(F)$. So $\Phi'(F) = -\nabla^2 F e^{\frac{z}{H}}$ which further implies that $\nabla^2 F e^{\frac{z}{H}}$ is a function of F and that $\nabla^2 F = \phi(F) e^{-\frac{z}{H}}$ where $\phi(F)$ is any function of F . Brown called this the basic equation for 2-dimensional static equilibrium. For a given $\phi(F)$ the solution F will give a field whose Lorentz force will balance plasma pressure and gravity.

Menzel's solution corresponds to $\phi(F) = A F^{1-\frac{2\hat{H}}{H}}$ where A and \hat{H} are constant and $F(x, z) = F(x) e^{-\frac{z}{2\hat{H}}}$. Dungey's solution is found with $\phi(F) = D$ where D is constant ($= \frac{1}{H^2}$ in Dungey's case), then $F(x, z) = D H^2 e^{-\frac{z}{H}} + f(x, z)$ where $f(x, z)$ is any harmonic function. Setting $\phi(F) = C e^{\frac{F}{G}}$, where $c < 0$ and G are constant and $F(x, z) = Gz + F(x)$ will reproduce the solution of Kippenhahn and Schlüter.

3.1.3 The Kuperus-Raadu Model

In 1974 a completely different type of prominence model was developed by Kuperus and Raadu [24]. They considered how plasma formations could develop in a current sheet (say between two active regions) and then be supported when the field lines reconnect. This topology can be considered as the sum of a simple open field with

straight field lines and a set of closed field lines, not tied to the photosphere, formed by superposition of the fields of two line currents (see figure 3.10) one above the photosphere (the prominence itself) and another an equal distance below the surface.

The KS and KR models have formed the basis for much work on quiescent solar prominences. Observational measurements show that most (75% to 90%) prominences are of the KR type [29]. Many other authors have extended these models. For example; Poland and Anzer [31] (1971) studied energy balance in the KS model, Ballester and Priest [32] (1987) modeled how the magnetic field would change with height in the KS model, Milne et al. [33] (1979) changed the angle the prominence normal makes with the horizontal magnetic field, Priest et al. [34] (1989) looked at three dimensional effects such as twisting of the magnetic field and Hood and Anzer [35] (1989) used typical measured values of the magnetic field along the prominence to extend the KS model. Others have developed their own models. Low [36] (1975), for example, considered both magnetostatic support and energy transport to create nonisothermal plasma sheets in the corona.

In my study of these models I found the KS model to be rather phenomenological in nature since the supporting field is simply placed in the corona. Although understood to be initially formed by currents in the convection zone and expelled through the photosphere there is no direct connection between the field in the corona and the convection. The KR model is more physical since the photospheric boundary is mimicked by a line current in the convection zone but a detailed field distribution is not specified. My aim was to generate magnetic fields in the corona directly from photospheric flows and convection. To do this it is necessary to introduce the subject

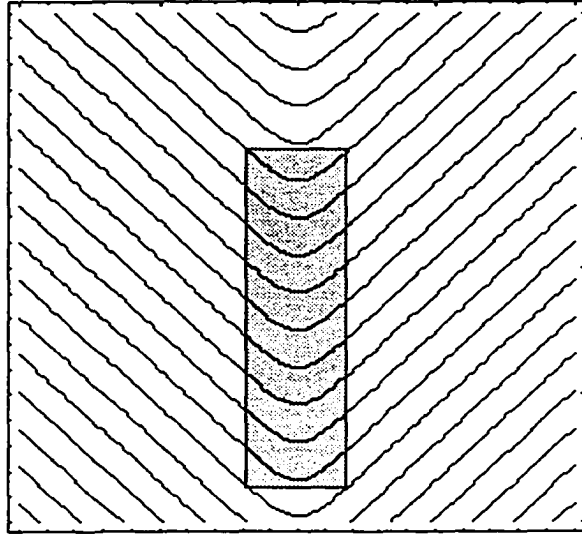


Fig. 3.9: Field lines of the Kippenhahn-Schlüter model.

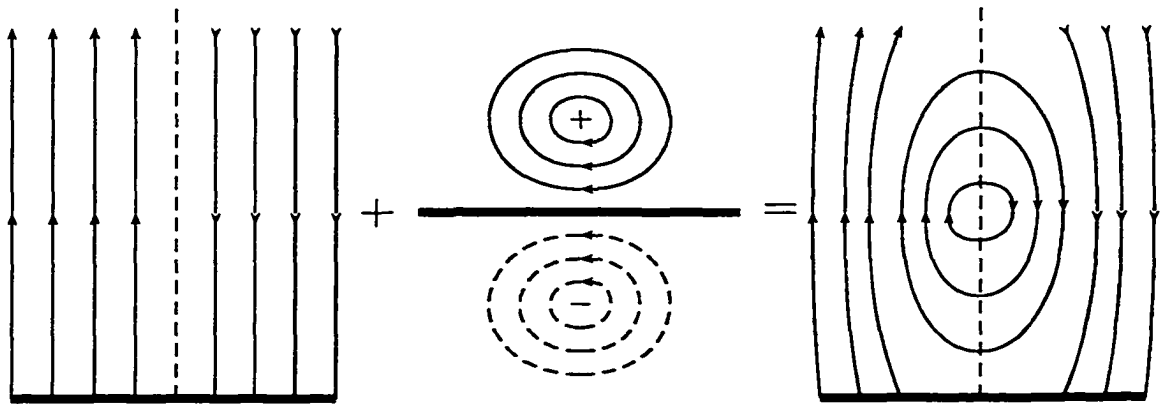


Fig. 3.10: The Kuperus-Raadu magnetic configuration.

of magnetoconvection.

3.2 Magnetoconvection

Convecting cells of plasma can generate, shape, amplify and expel magnetic fields. In dynamical magnetoconvection both the fluid velocity and the magnetic field are allowed to interact. The resulting equations are nonlinear and often require supercomputers to solve them numerically. However, if we assume that the magnetic energy is small compared to the kinetic energy of the fluid (i.e. $\frac{B^2}{2\mu} \ll \frac{1}{2}\rho v^2$, a good approximation in the photosphere) then we can enter the linear realm of kinematical magnetoconvection. Here a steady fluid velocity is prescribed and its effect on the magnetic field computed; the magnetic field however does not influence the velocity. The basic equation is the induction equation:

$$\frac{\partial \vec{B}}{\partial t} = \nabla \times (\vec{v} \times \vec{B}) + \eta \nabla^2 \vec{B}.$$

Parker [37] (1963) found exact solutions to this equation on both infinite and semi-infinite intervals for various flows \vec{v} , and included both time-dependent and steady-state cases. An example that will be of interest later is the velocity field given by the stream function $\Psi(x, y) = -e^{-y} \sin x$ on $-2\pi \leq x \leq 2\pi$ and $-\infty < y < \infty$. This velocity field represents a stationary convective upwelling, a convection cell. A steady state solution was sought ($\frac{\partial}{\partial t} \equiv 0$) with periodic boundary conditions in x and $\vec{B} = \langle B_0, 0, 0 \rangle$ as $y \rightarrow \infty$. He obtained the solution $\vec{B} = \nabla \times \langle 0, 0, A \rangle$ where $A(x, y) = B_0 \exp(-\frac{1}{2}e^{-y} \cos x) K_0(\frac{1}{2}e^{-y})$ (see figure 3.11). Note how the magnetic flux is expelled from the upwelling region and concentrated in the downflow.

Weiss [38] (1966) numerically solved the induction equation over finite domains at various Reynolds numbers. Initially uniform fields were ejected from regions of high fluid velocity and concentrated at the boundaries which were assumed to be perfectly conducting - which ties the field lines to the boundary and confines it to the region of fluid flow. Even the time-dependent case reached a steady state. Weiss used a variety of convection patterns from a single isolated eddy to multiple convection cells. At low Reynolds numbers, the field was concentrated at the edges but some field lines remained in the convection cell. At higher Reynolds numbers, reconnection took place in the center of the cell and a majority of the flux was concentrated at the boundary. See figure 3.12 for an example of flux being expelled from a convection cell. For a comprehensive review of magnetoconvection see [39] and [40].

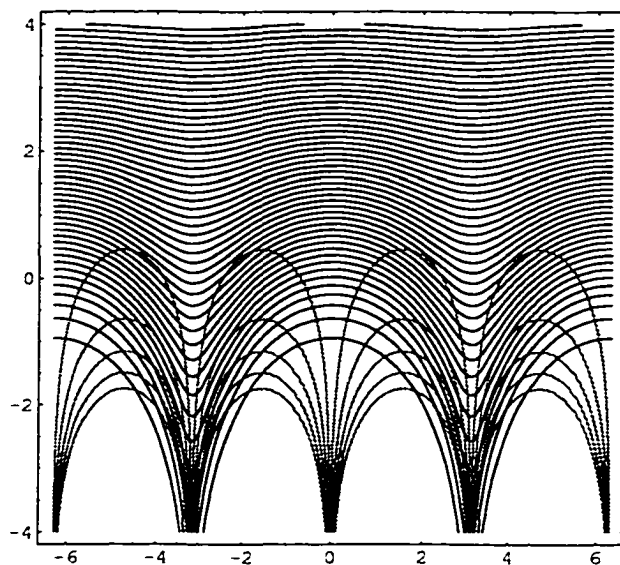


Fig. 3.11: One of Parker's solutions to the steady state induction equation. The light lines are the streamlines of the fluid, and the darker lines represent the magnetic field.

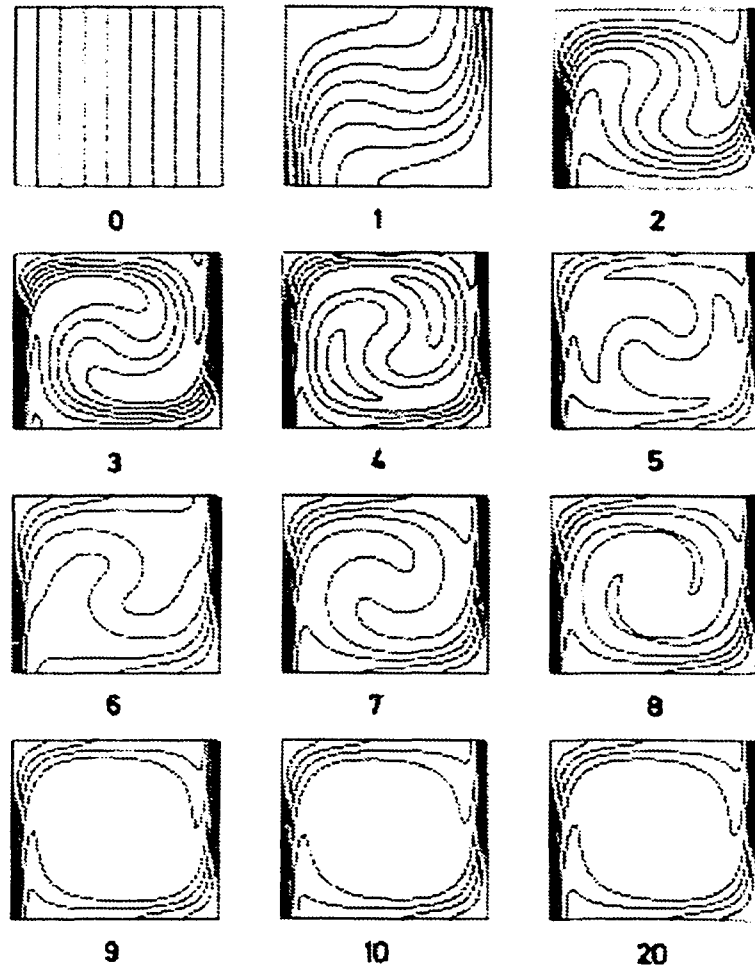


Fig. 3.12: The expulsion of magnetic flux from a convection cell.

reproduced with permission of Dr. N.O. Weiss

CHAPTER 4

SOLAR PROMINENCE MAGNETIC CONFIGURATIONS AND CONVECTION

4.1 A Dirichlet Problem with Applications to Solar Prominences

Before tackling the full two-dimensional convection problem, a simpler case was considered. The convection was simulated only at the photosphere by a one-dimensional boundary condition that will generate a potential magnetic field in a region free of current. This is a special case of a force free field ($\nabla \times \vec{B} = \alpha \vec{B}$) with $\alpha = 0$. The equation to be solved is then $\nabla \times \vec{B} = \vec{0}$ on a semi-infinite strip $|x| \leq L, y \geq 0$, the region above the convection cell. The two-dimensional problem can be simplified with the introduction of a vector potential $A(x, y)$ for \vec{B} , otherwise known as a flux function. Then $\vec{B} = \nabla \times \langle 0, 0, A \rangle = \langle \frac{\partial A}{\partial y}, -\frac{\partial A}{\partial x}, 0 \rangle$ and the magnetic lines of force are given by the contours of A . In terms of A the boundary value problem becomes:

$$\nabla^2 A(x, y) = 0$$

with boundary conditions,

$$A(L, y) = g_1(y)$$

$$A(-L, y) = g_2(y)$$

$$A(x, 0) = f(x).$$

This problem can be solved by conformal mapping and then using the method of images. Laplace's equation is invariant under a conformal mapping and the transformation $w = \sin \frac{\pi}{2L} z$ where $z = x + iy$ and $w = u + iv$ maps the semi-infinite region into the half-plane $-\infty < u < \infty, v \geq 0$ (see figure 4.1) [41]. In terms of u and v the problem becomes:

$$\nabla^2 A(u, v) = 0$$

with boundary conditions,

$$A(u, 0) = \begin{cases} \bar{g}_2(u) & , \quad u < -1 \\ \bar{f}(u) & , \quad -1 < u < 1 \\ \bar{g}_1(u) & , \quad u > 1, \end{cases}$$

a problem that can be solved by the method of images – using infinite space Green's functions to obtain solutions on semi-infinite intervals. Details of this method can be found in [42] but a brief review is given as an appendix. The solution is:

$$A(u, v) = \frac{v}{\pi} \int_{-\infty}^{\infty} \frac{A(s, 0)}{(s - u)^2 + v^2} ds.$$

Transforming back to the xy -plane we find:

$$A(x, y) = \frac{v}{\pi} \left[\int_{-\infty}^{-1} \frac{\bar{g}_2(s)}{(s - u)^2 + v^2} ds + \int_{-1}^1 \frac{\bar{f}(s)}{(s - u)^2 + v^2} ds + \int_1^{\infty} \frac{\bar{g}_1(s)}{(s - u)^2 + v^2} ds \right]$$

where,

$$u = \sin\left(\frac{\pi}{2L}x\right) \cosh\left(\frac{\pi}{2L}y\right)$$

$$v = \cos\left(\frac{\pi}{2L}x\right) \sinh\left(\frac{\pi}{2L}y\right)$$

$$\bar{f}(s) = f\left(\frac{2L}{\pi} \sin^{-1} s\right)$$

$$\bar{g}_1(s) = g_1\left(\frac{2L}{\pi} \cosh^{-1} s\right)$$

$$\bar{g}_2(s) = g_2\left(\frac{2L}{\pi} \cosh^{-1}(-s)\right).$$

If we assume complete symmetry about $x = 0$, i.e. $g_1(y) = g_2(y) = g(y)$ and $f(-x) = f(x)$, then the solution can be reduced to:

$$A(x, y) = \frac{v}{\pi} \left[\int_{-1}^1 \frac{\tilde{f}(s)}{(s-u)^2 + v^2} ds + \int_1^\infty \frac{\tilde{g}(s)}{(s+u)^2 + v^2} + \frac{\tilde{g}(s)}{(s-u)^2 + v^2} ds \right]$$

where,

$$u = \sin\left(\frac{\pi}{2L}x\right) \cosh\left(\frac{\pi}{2L}y\right)$$

$$v = \cos\left(\frac{\pi}{2L}x\right) \sinh\left(\frac{\pi}{2L}y\right)$$

$$\tilde{f}(s) = f\left(\frac{2L}{\pi} \sin^{-1} s\right)$$

$$\tilde{g}(s) = g\left(\frac{2L}{\pi} \cosh^{-1} s\right).$$

Let's first examine some cases where the integrals can be found analytically. One such case is $f(x) = \alpha$ and $g(y) = \beta$ where α and β are constants. The integrals are inverse tangent functions and use of the trigonometric identity $\tan(\theta + \phi) = \frac{\tan \theta + \tan \phi}{1 - \tan \theta \tan \phi}$ gives the solution:

$$A(x, y) = \frac{2}{\pi}(\alpha - \beta) \tan^{-1} \left[\frac{\cos\left(\frac{\pi}{2L}x\right)}{\sinh\left(\frac{\pi}{2L}y\right)} \right] + \beta.$$

A contour plot of A with $L = \frac{\pi}{2}$, $\alpha = 1$ and $\beta = 0$ (see figure 4.2) gives simple magnetic arches – which could be a KS type configuration before any plasma has condensed to bend the field lines.

Another case that can be integrated exactly is $f(x) = |\sin(\frac{\pi}{2L}x)|$ and $g(y) = 0$. This is a photospheric potential that is weak at the center and gets stronger toward the edges of the cell. The integrals here can be written as inverse tangent functions and natural logarithms, and after using several trigonometric identities, becomes:

$$A(x, y) = \frac{2}{\pi} \sin\left(\frac{\pi}{2L}x\right) \cosh\left(\frac{\pi}{2L}y\right) \tan^{-1} \left[\frac{\sin\left(\frac{\pi}{2L}x\right) \cos\left(\frac{\pi}{2L}x\right)}{\sinh\left(\frac{\pi}{2L}y\right) \cosh\left(\frac{\pi}{2L}y\right)} \right] + \frac{1}{2\pi} \cos\left(\frac{\pi}{2L}x\right) \sinh\left(\frac{\pi}{2L}y\right) \ln \left[\frac{\cos\left(\frac{\pi}{L}x\right) + \cosh\left(\frac{\pi}{L}y\right)}{\cos\left(\frac{\pi}{L}x\right) - \cosh\left(\frac{\pi}{L}y\right)} \right]^2,$$

whose contour plot (again with $L = \frac{\pi}{2}$) is figure 4.3.

A photospheric potential that is strong at the center and weak at the edges is $f(x) = \cos(\frac{\pi}{2L}x)$. The integrals here have to be evaluated numerically. This was done on Mathematica using the `NIntegrate` and `ListContourPlot` commands. With $L = \frac{\pi}{2}$ the field lines again resemble magnetic arches (see figure 4.4).

Here are some cases where $g(y) \neq 0$. Figures 4.5 and 4.6 are $f(x) = |\sin x|$ and $f(x) = 1$ respectively, both with $g(y) = \begin{cases} 1 & , 0 < y < .5 \\ 0 & , y > .5 \end{cases}$. Note how the field lines bunch together at the edges to form “feet”.

4.2 Solar Prominence Magnetic Configurations Derived Numerically from Convection

The Dirichlet problem shows that prominence type fields can be generated by photospheric motions, but the photosphere is just the visible top of the convection zone. It would be more physically realistic if two-dimensional convection could be used to expel magnetic flux into the corona. To this end we examine the induction equation. We want a solution that will satisfy this equation below the photosphere, where the primary physics is that of fluid convection, and be a current free field in the corona where there is no plasma motion (see figure 4.7). We will require that any solution match at the photosphere ($y = 0$).

The photosphere is assumed to be non-conducting so magnetic flux can be expelled from the convection zone into the corona, and that enough time has elapsed in order that a steady solution has been reached. We introduce the same vector potential

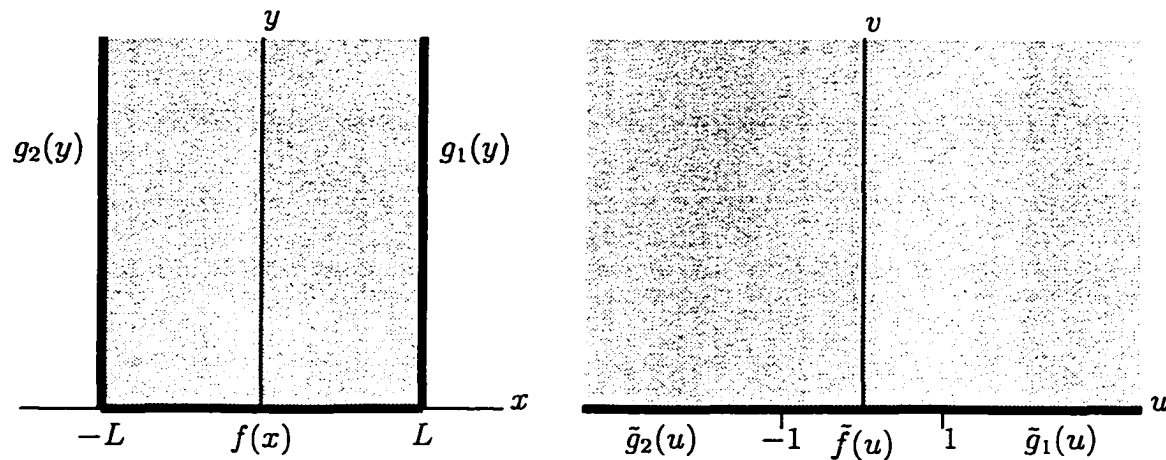


Fig. 4.1: The xy and uv planes.

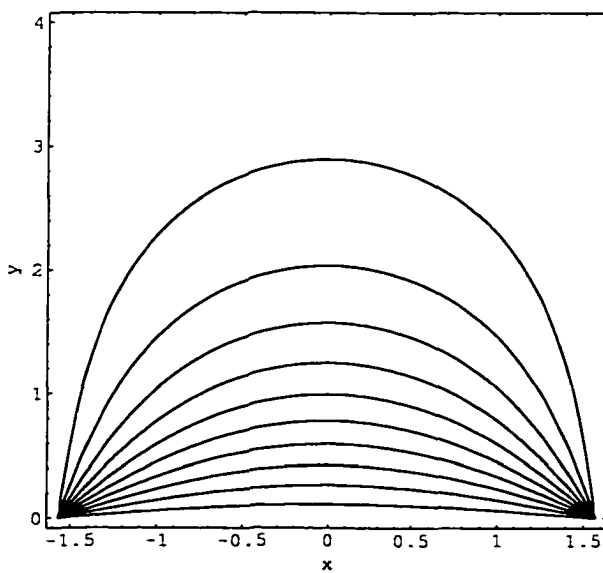


Fig. 4.2: $f(x) = 1$ and $g(y) = 0$.

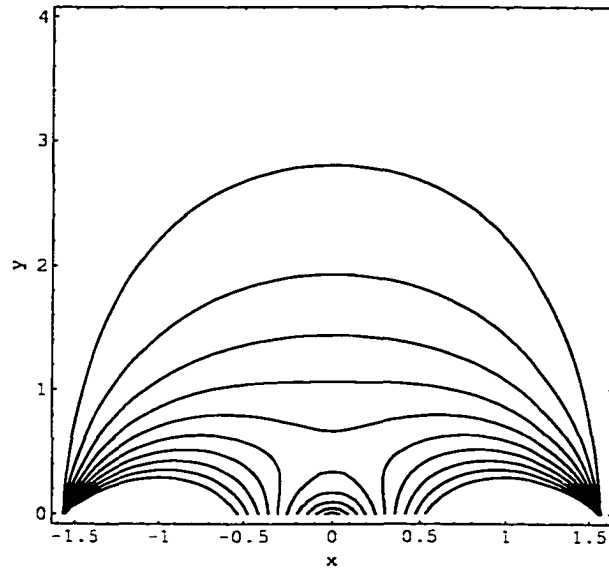


Fig. 4.3: $f(x) = |\sin x|$ and $g(y) = 0$.

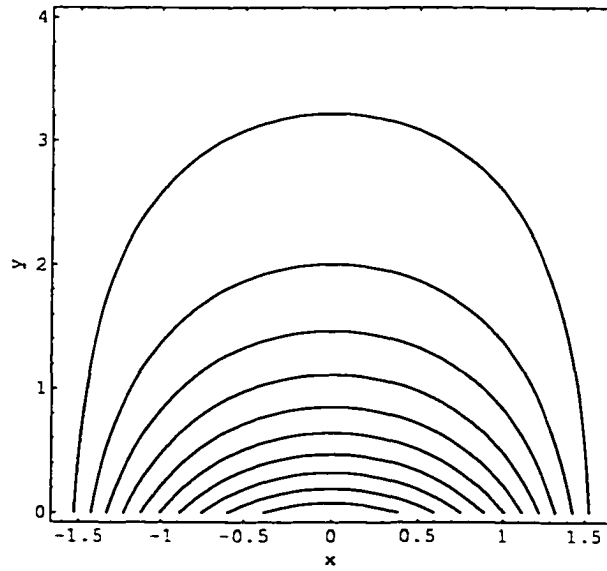


Fig. 4.4: $f(x) = \cos x$ and $g(y) = 0$.

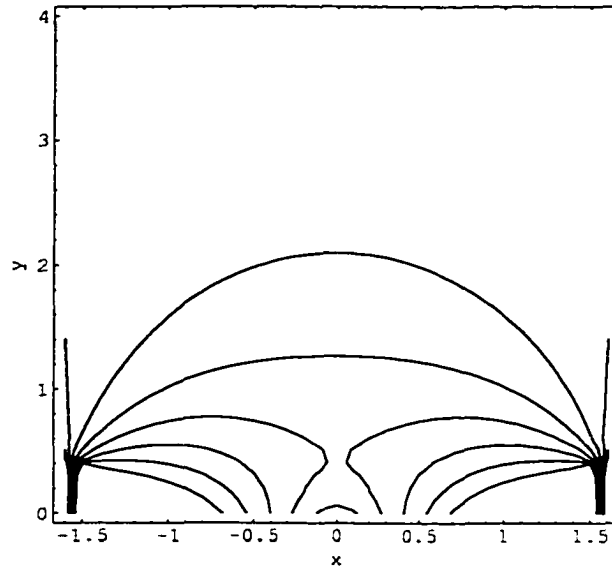


Fig. 4.5: $f(x) = |\sin x|$ and $g(y) = \begin{cases} 1, & 0 < y < .5 \\ 0, & y > .5 \end{cases}$.

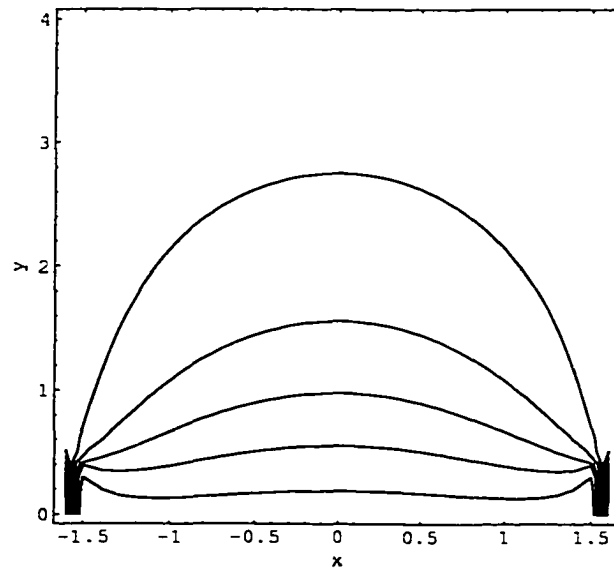


Fig. 4.6: $f(x) = 1$ and $g(y) = \begin{cases} 1, & 0 < y < .5 \\ 0, & y > .5 \end{cases}$.

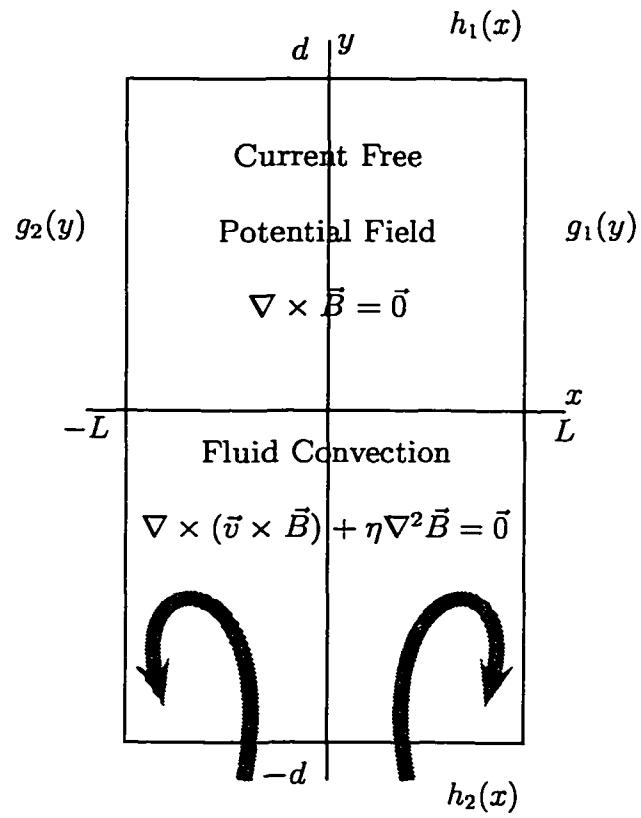


Fig. 4.7: The xy -plane.

$A(x, y)$ as before which gives Laplace's equation, $\nabla^2 A = 0$, in the region $y > 0$. In the region $y < 0$ the steady state induction equation becomes a diffusion equation with convection terms:

$$v_1(x, y) \frac{\partial A}{\partial x} + v_2(x, y) \frac{\partial A}{\partial y} - \eta \nabla^2 A = 0.$$

where $\vec{v} = \langle v_1, v_2 \rangle$ will be specified. The computational box will be $-L < x < L$ and $-d < y < d$ with boundary conditions specified as $g_1(y)$ and $g_2(y)$ on $x = L$ and $x = -L$ respectively, and $h_1(x)$ and $h_2(x)$ on $y = d$ and $y = -d$ respectively.

To eliminate the first derivative terms and aid in matching the solutions on $y = 0$ we first make the transformation $A = \Lambda(x, y)e^{H(x, y)}$ where $H = \frac{\phi}{2\eta}$ and $\phi(x, y)$ is the velocity potential (i.e. $\vec{v} = \nabla\phi$). This yields a Helmholtz equation:

$$\eta \nabla^2 \Lambda + f(x, y) \Lambda = 0$$

where

$$f(x, y) = \frac{1}{4} \left[2 \left(\frac{\partial v_1}{\partial x} + \frac{\partial v_2}{\partial y} \right) - \frac{1}{\eta} (v_1^2 + v_2^2) \right].$$

We have restricted \vec{v} to conservative flows only (i.e. those where $\nabla \times \vec{v} = \vec{0}$), but by setting $f(x, y) \equiv 0$ in the region $y > 0$ we force the two solutions to match at the photosphere. This follows even though $\nabla^2 A$ does not become Laplace's equation in terms of Λ but the more complicated version:

$$\eta \nabla^2 \Lambda + \left[\frac{1}{4\eta} (v_1^2 + v_2^2) + \frac{1}{2} \left(\frac{\partial v_1}{\partial x} + \frac{\partial v_2}{\partial y} \right) \right] \Lambda + v_1 \frac{\partial \Lambda}{\partial x} + v_2 \frac{\partial \Lambda}{\partial y} = 0.$$

This equation does reduce to $\nabla^2 \Lambda = 0$ in the corona since $\vec{v} \equiv \vec{0}$ there (also note that $\vec{v} \equiv \vec{0} \Rightarrow \phi = \text{constant} \Rightarrow H = \text{constant} \Rightarrow \nabla^2 \Lambda = 0$). Since this transformation

eliminates the first derivative terms there is no need to approximate them, making the numerical scheme more efficient and accurate.

Even though the equations match at the photosphere ($y = 0$) when $f(x, y) \equiv 0$ there is still the question of continuity in the magnetic field. To examine this, we look at the jump in \vec{B} across $y = 0$. Since $\vec{B} = \langle \frac{\partial A}{\partial y}, -\frac{\partial A}{\partial x} \rangle$ where $A = \Lambda e^{\frac{\phi}{2\eta}}$ we find (letting $\phi \equiv 0$ for $y > 0$ to force no flow in the corona):

$$[\vec{B}] = \left\langle (e^{\frac{\phi}{2\eta}} - 1) \frac{\partial \Lambda}{\partial y} + \frac{\Lambda}{2\eta} \frac{\partial \phi}{\partial y} e^{\frac{\phi}{2\eta}}, -(e^{\frac{\phi}{2\eta}} - 1) \frac{\partial \Lambda}{\partial x} - \frac{\Lambda}{2\eta} \frac{\partial \phi}{\partial x} e^{\frac{\phi}{2\eta}} \right\rangle.$$

From this it can be seen that sufficient conditions for the jump in the tangential component (to the photosphere) to be zero are ϕ and $\frac{\partial \phi}{\partial y} \rightarrow 0$ as $y \rightarrow 0$, and for the jump in the normal component to be zero ϕ and $\frac{\partial \phi}{\partial x} \rightarrow 0$ as $y \rightarrow 0$. These conditions form a special class of velocity flows that will force either (or both) of the magnetic field components to be continuous at $y = 0$. However, it is not necessary to restrict the velocity to this type of flow. A discontinuity in either component creates a current sheet whose diffusion will be counteracted by the convection term in the induction equation. Accepting such a discontinuity is not without precedent. For example, in modeling running penumbral waves in sunspots Nye and Thomas [3] used a two layer model where a horizontal magnetic field was placed above a region of zero magnetic field.

The numerical method used was the finite difference method [43]. The computational box was discretized into an $n \times m$ mesh and the second partial derivatives were

approximated by a central difference scheme:

$$\Lambda_{xx} \approx \frac{\Lambda(x_{i+1}, y_j) - 2\Lambda(x_i, y_j) + \Lambda(x_{i-1}, y_j)}{h^2}$$

$$\Lambda_{yy} \approx \frac{\Lambda(x_i, y_{j+1}) - 2\Lambda(x_i, y_j) + \Lambda(x_i, y_{j-1})}{k^2}$$

where $h = \frac{2L}{n}$ and $k = \frac{2d}{m}$. Each interior mesh point (x_i, y_j) uses its four neighboring points to form an equation. Substituting the above approximations for the second partials into the Helmholtz equation and using $\omega_{i,j} \approx \Lambda(x_i, y_j)$, we obtain the difference-equation:

$$k^2 [\omega_{i+1,j} - 2\omega_{i,j} + \omega_{i-1,j}] + h^2 [\omega_{i,j+1} - 2\omega_{i,j} + \omega_{i,j-1}] + \frac{h^2 k^2}{\eta} f(x_i, y_j) \omega_{i,j} = 0$$

where

$$i = 1, \dots, n - 1$$

$$j = 1, \dots, m - 1,$$

and the boundary conditions give:

$$\omega_{0,j} = g_2(y_j) \quad , \quad j = 0, \dots, m$$

$$\omega_{n,j} = g_1(y_j) \quad , \quad j = 0, \dots, m$$

$$\omega_{i,0} = h_2(x_i) \quad , \quad i = 1, \dots, n - 1$$

$$\omega_{i,n} = h_1(x_i) \quad , \quad i = 1, \dots, n - 1.$$

This yields an $(n - 1)(m - 1) \times (n - 1)(m - 1)$ linear system. The scheme was programmed on Mathematica taking advantage of its extensively tested subroutine LinearSolve for solving the large linear systems created by the finite difference method. Once the solution for $\Lambda(x, y)$ was found it was multiplied by $e^{\frac{\phi}{2\eta}}$ to obtain $A(x, y)$. A contour plot of A then gives the magnetic field lines. The Mathematica code is given as an appendix.

All the runs were made with $L = 6.3 \approx 2\pi$, $d = 4$ and $n = m = 40$. Two stream functions were used (see figures 4.8 and 4.9): $\Psi_1(x, y) = -\sin x \sinh y$, and $\Psi_2(x, y) = -e^{-y} \sin x$. Figures 4.10 through 4.20 are Ψ_1 with various boundary conditions and figures 4.21 through 4.31 are Ψ_2 with the same set of boundary conditions. Note that figures 4.22, 4.23, 4.26 and 4.27 resemble Parker's analytic solution.

The main results of this chapter were published in *Astronomy & Astrophysics* [44, 45]. Since $\|\vec{B}\| = \sqrt{\left(\frac{\partial A}{\partial x}\right)^2 + \left(\frac{\partial A}{\partial y}\right)^2}$, and the partials can be computed from the matrix A , the strength of the magnetic field along the contour lines could be found numerically. These values could then be compared to actual prominence field measurements. This could be an addendum to [45].

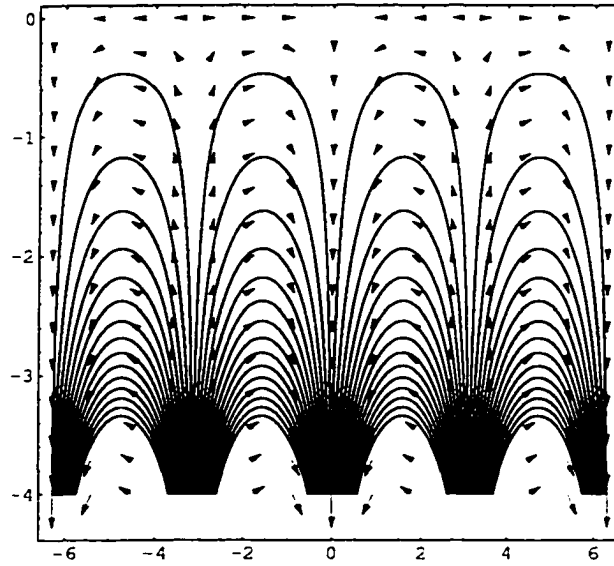


Fig. 4.8: The stream function $\Psi_1(x, y) = -\sin x \sinh y$. A deep convection cell with a downflow at the center.

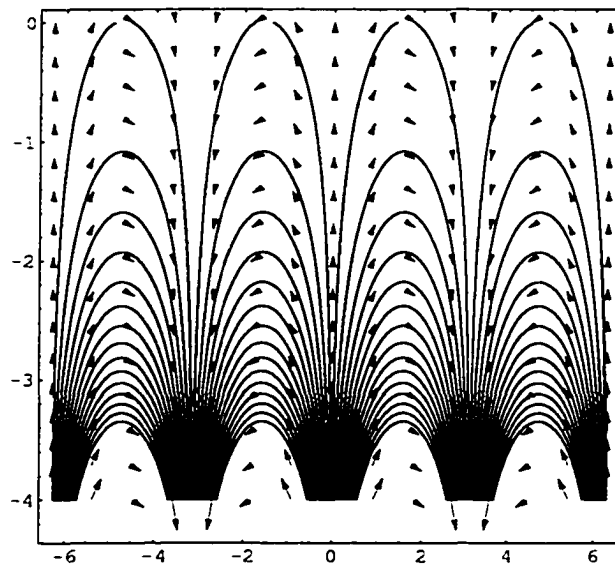


Fig. 4.9: The stream function $\Psi_2(x, y) = -e^{-y} \sin x$. A deep convection cell with an upflow in the center.

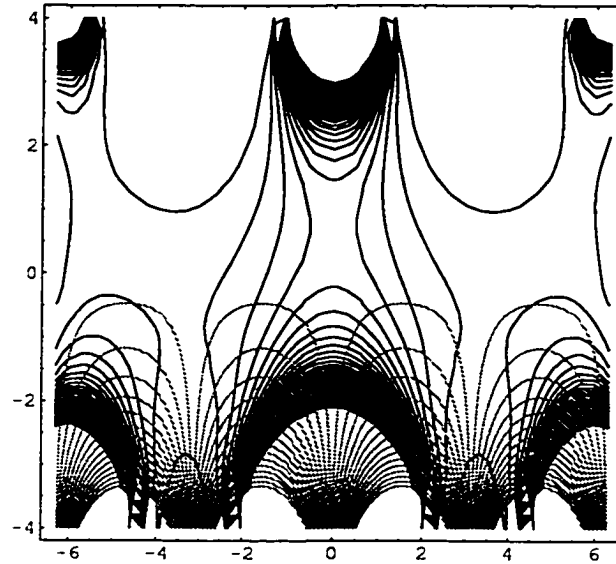


Fig. 4.10: The stream function Ψ_1 (light lines) and the magnetic field lines with $g_1(y) = g_2(y) = 0$ and $h_1(x) = 0, h_2(x) = 100$

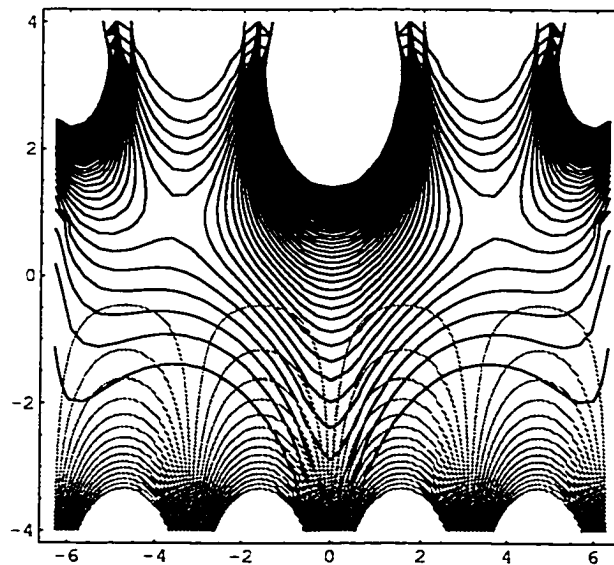


Fig. 4.11: The stream function Ψ_1 (light lines) and the magnetic field lines with $g_1(y) = g_2(y) = 0$ and $h_1(x) = 100, h_2(x) = 0$

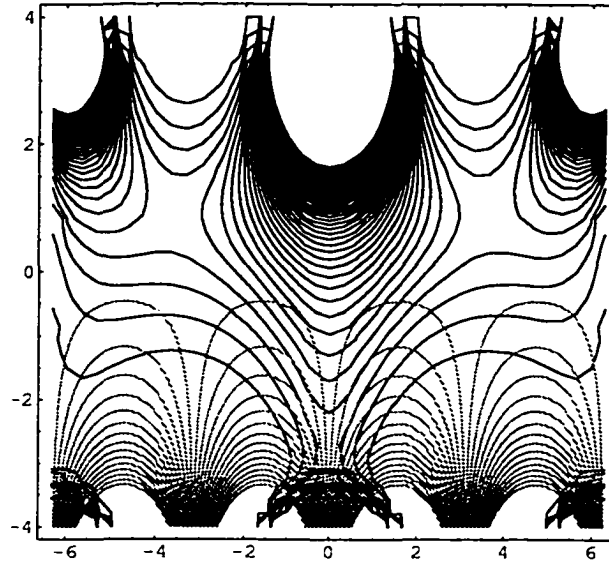


Fig. 4.12: The stream function Ψ_1 (light lines) and the magnetic field lines with $g_1(y) = g_2(y) = 0$ and $h_1(x) = 100, h_2(x) = 100$

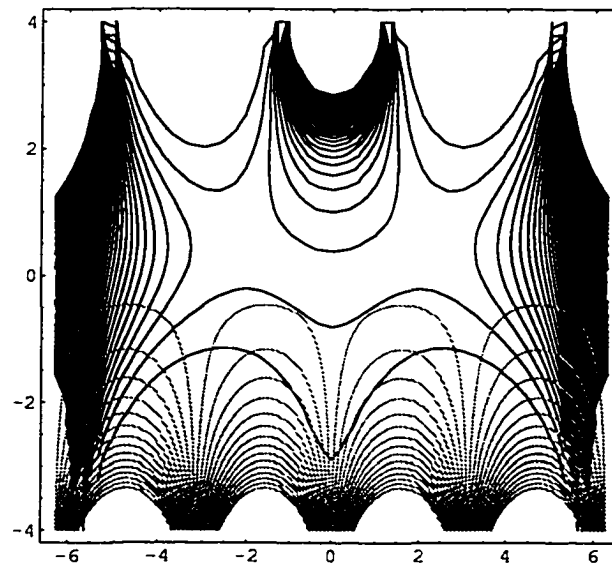


Fig. 4.13: The stream function Ψ_1 (light lines) and the magnetic field lines with $g_1(y) = g_2(y) = 100$ and $h_1(x) = 0, h_2(x) = 0$

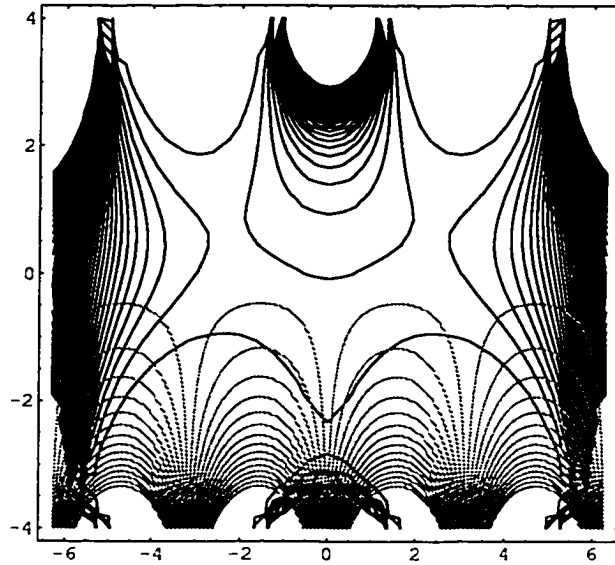


Fig. 4.14: The stream function Ψ_1 (light lines) and the magnetic field lines with $g_1(y) = g_2(y) = 100$ and $h_1(x) = 0, h_2(x) = 100$

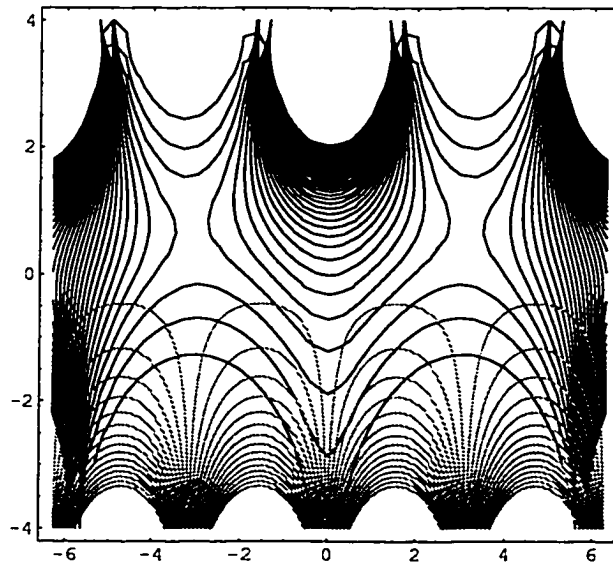


Fig. 4.15: The stream function Ψ_1 (light lines) and the magnetic field lines with $g_1(y) = g_2(y) = 100$ and $h_1(x) = 100, h_2(x) = 0$

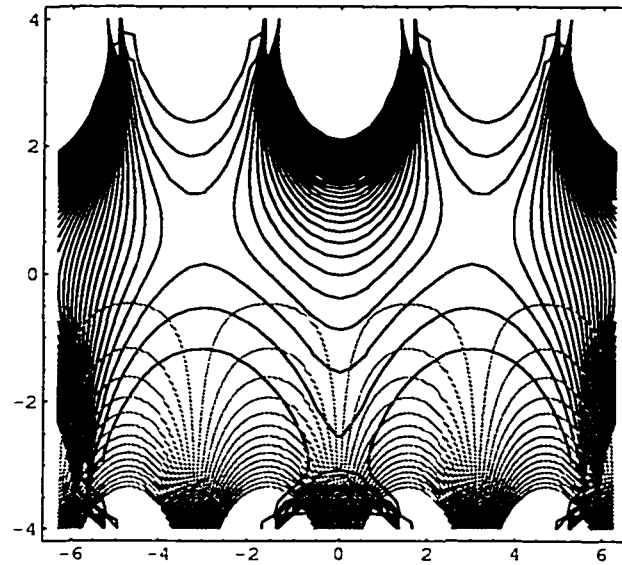


Fig. 4.16: The stream function Ψ_1 (light lines) and the magnetic field lines with $g1(y) = g2(y) = 100$ and $h1(x) = 100, h2(x) = 100$

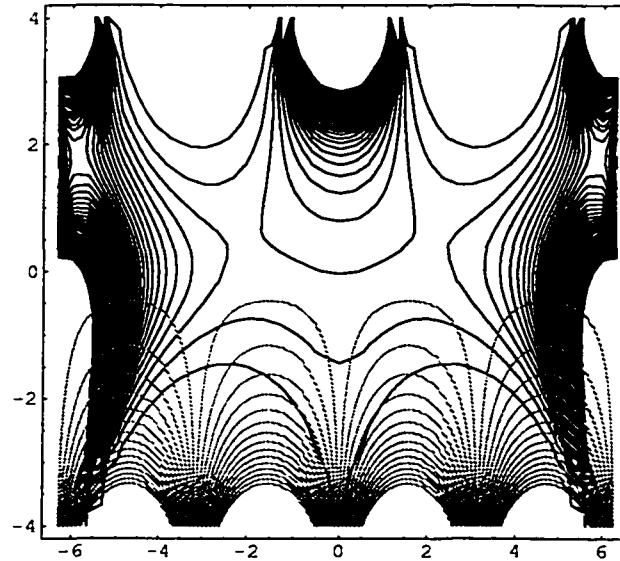


Fig. 4.17: The stream function Ψ_1 (light lines) and the magnetic field lines with $g1(y) = g2(y) = \begin{cases} 100 & , y < 0 \\ 0 & , y > 0 \end{cases}$ and $h1(x) = 0, h2(x) = 0$

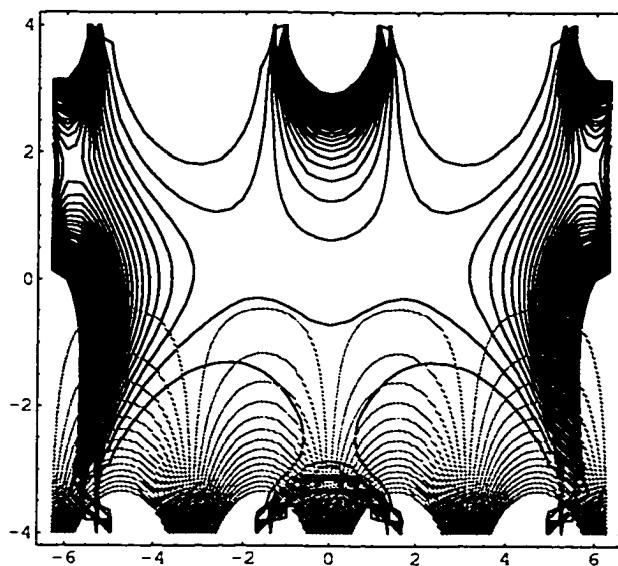


Fig. 4.18: The stream function Ψ_1 (light lines) and the magnetic field lines with

$$g1(y) = g2(y) = \begin{cases} 100 & , y < 0 \\ 0 & , y > 0 \end{cases} \quad \text{and } h1(x) = 0, h2(x) = 100$$

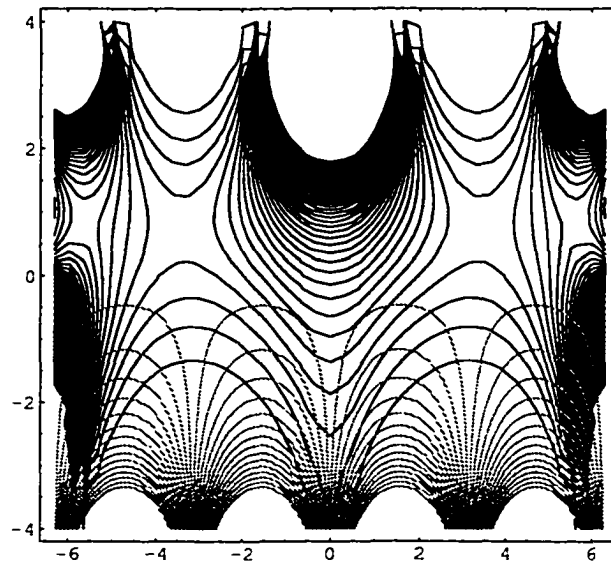


Fig. 4.19: The stream function Ψ_1 (light lines) and the magnetic field lines with

$$g_1(y) = g_2(y) = \begin{cases} 100 & , y < 0 \\ 0 & , y > 0 \end{cases} \quad \text{and } h_1(x) = 100, h_2(x) = 0$$

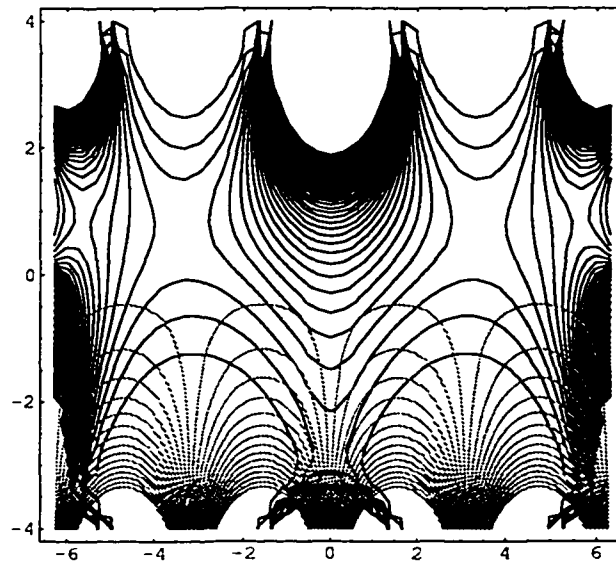


Fig. 4.20: The stream function Ψ_1 (light lines) and the magnetic field lines with

$$g_1(y) = g_2(y) = \begin{cases} 100 & , y < 0 \\ 0 & , y > 0 \end{cases} \quad \text{and } h_1(x) = 100, h_2(x) = 100$$

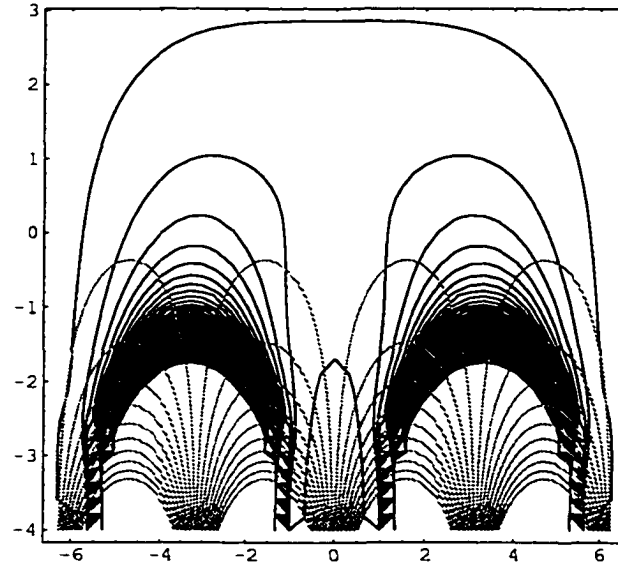


Fig. 4.21: The stream function Ψ_2 (light lines) and the magnetic field lines with $g_1(y) = g_2(y) = 0$ and $h_1(x) = 0, h_2(x) = 100$

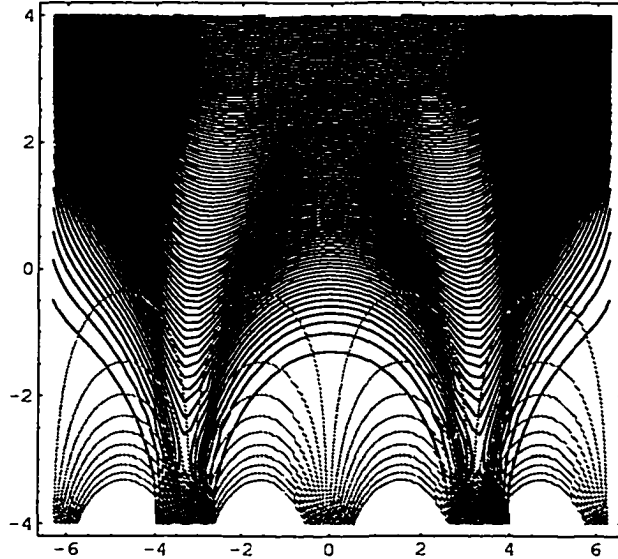


Fig. 4.22: The stream function Ψ_2 (light lines) and the magnetic field lines with $g_1(y) = g_2(y) = 0$ and $h_1(x) = 100, h_2(x) = 0$

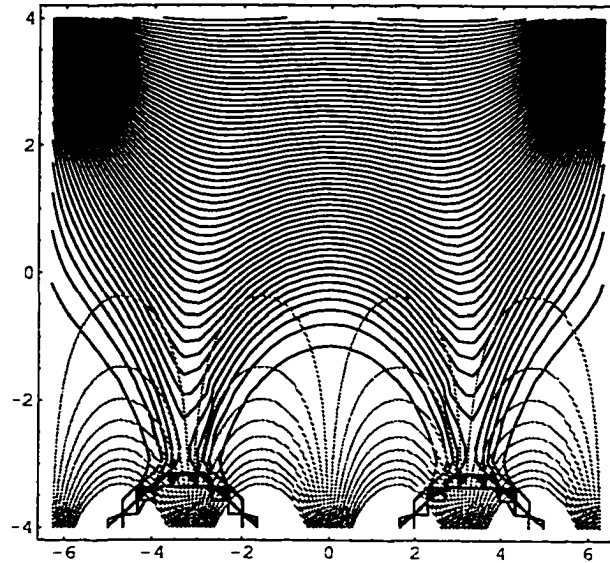


Fig. 4.23: The stream function Ψ_2 (light lines) and the magnetic field lines with $g_1(y) = g_2(y) = 0$ and $h_1(x) = 100, h_2(x) = 100$

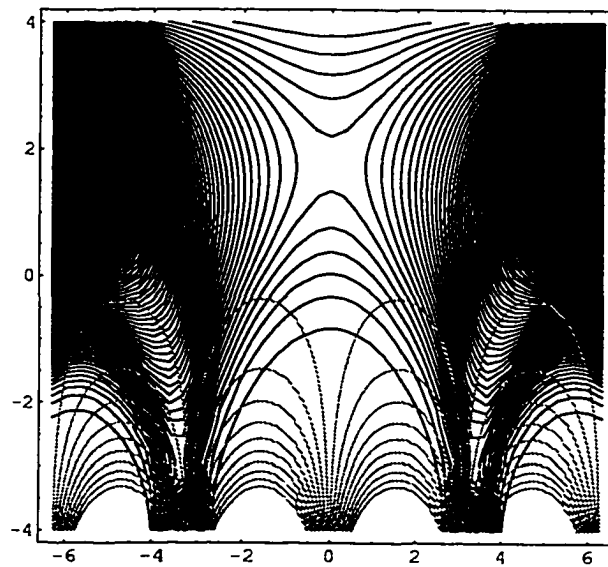


Fig. 4.24: The stream function Ψ_2 (light lines) and the magnetic field lines with $g_1(y) = g_2(y) = 100$ and $h_1(x) = 0, h_2(x) = 0$

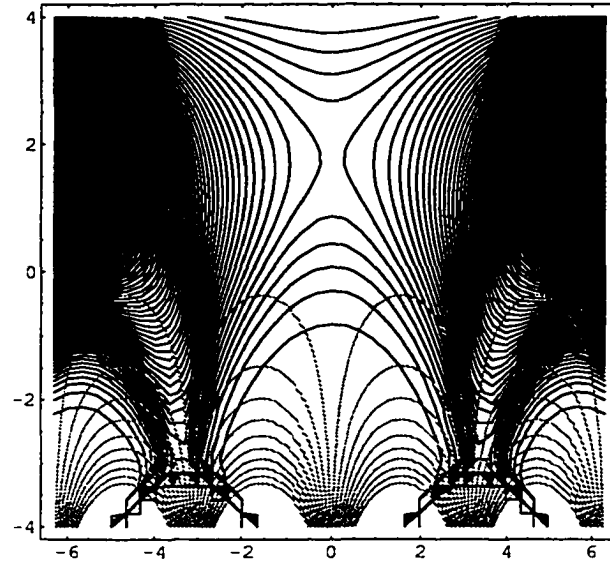


Fig. 4.25: The stream function Ψ_2 (light lines) and the magnetic field lines with $g_1(y) = g_2(y) = 100$ and $h_1(x) = 0, h_2(x) = 100$

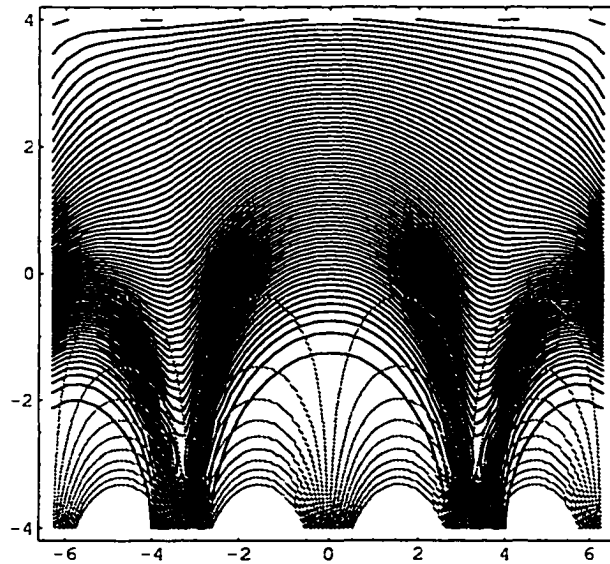


Fig. 4.26: The stream function Ψ_2 (light lines) and the magnetic field lines with $g_1(y) = g_2(y) = 100$ and $h_1(x) = 100, h_2(x) = 0$

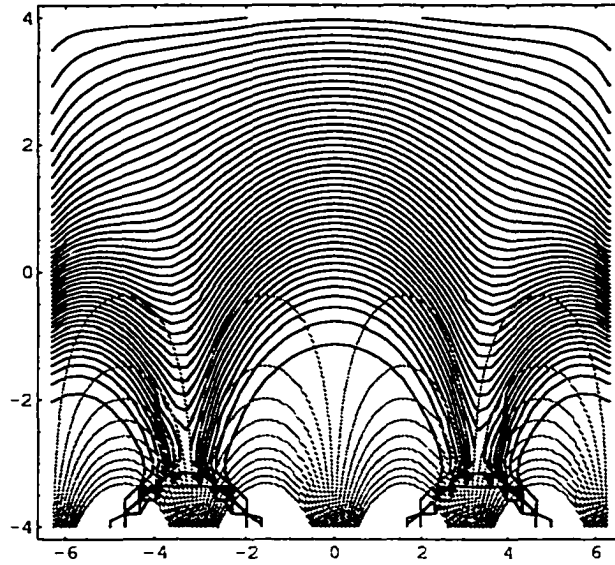


Fig. 4.27: The stream function Ψ_2 (light lines) and the magnetic field lines with $g_1(y) = g_2(y) = 100$ and $h_1(x) = 100, h_2(x) = 100$

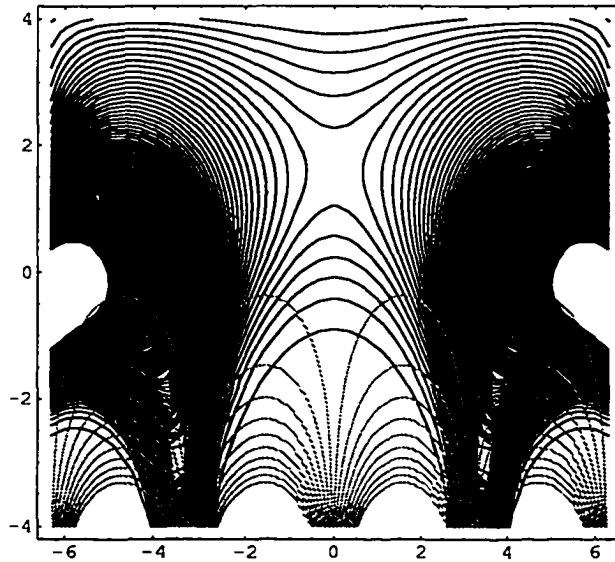


Fig. 4.28: The stream function Ψ_2 (light lines) and the magnetic field lines with $g_1(y) = g_2(y) = \begin{cases} 100 & , y < 0 \\ 0 & , y > 0 \end{cases}$ and $h_1(x) = 0, h_2(x) = 0$

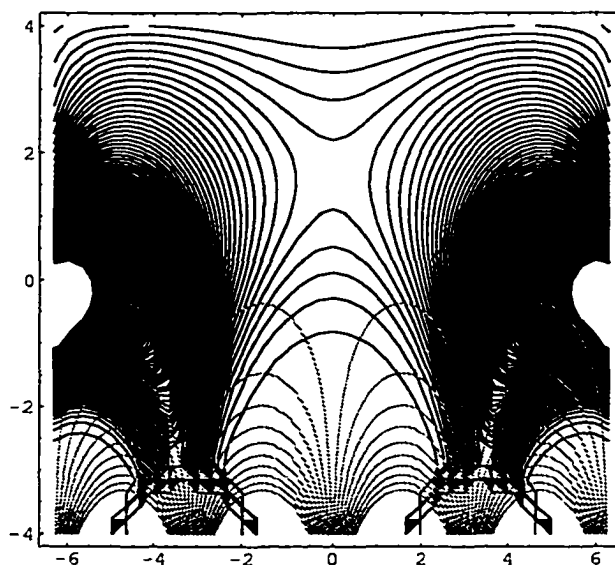


Fig. 4.29: The stream function Ψ_2 (light lines) and the magnetic field lines with

$$g1(y) = g2(y) = \begin{cases} 100 & , y < 0 \\ 0 & , y > 0 \end{cases} \quad \text{and } h1(x) = 0, h2(x) = 100$$

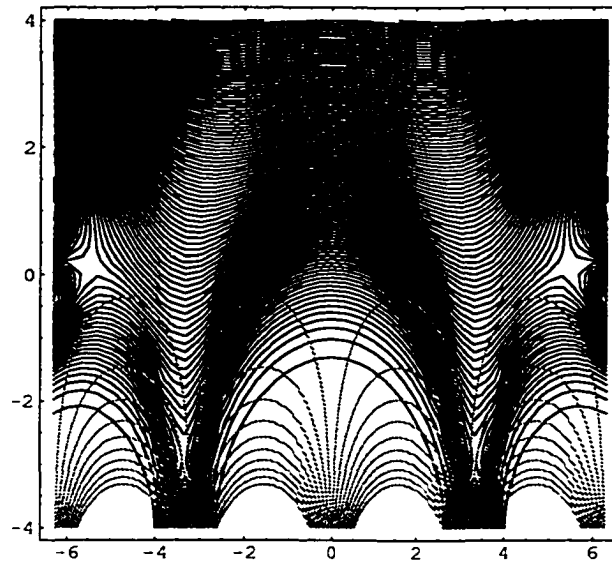


Fig. 4.30: The stream function Ψ_2 (light lines) and the magnetic field lines with

$$g_1(y) = g_2(y) = \begin{cases} 100 & , y < 0 \\ 0 & , y > 0 \end{cases} \quad \text{and } h_1(x) = 100, h_2(x) = 0$$

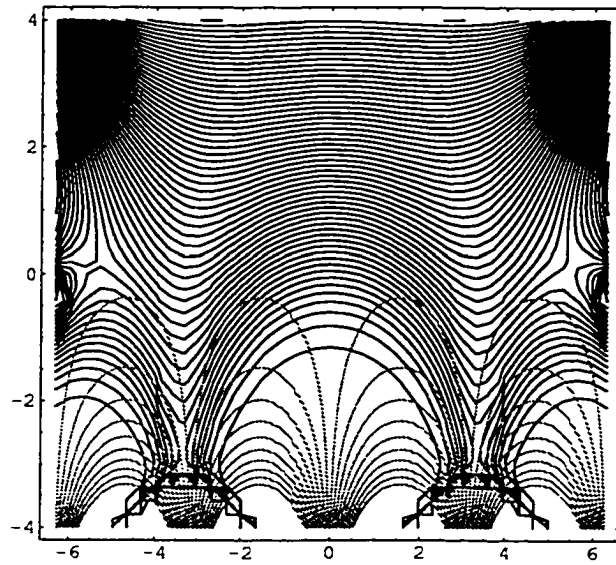


Fig. 4.31: The stream function Ψ_2 (light lines) and the magnetic field lines with

$$g_1(y) = g_2(y) = \begin{cases} 100 & , y < 0 \\ 0 & , y > 0 \end{cases} \quad \text{and } h_1(x) = 100, h_2(x) = 100$$

CHAPTER 5

CONCLUSION

The object of this thesis has been to show that the solar convection zone can be a driving force that expels magnetic flux into the solar atmosphere with the requisite topology needed to form quiescent prominences. Both problems solved have shown that this is possible. The solutions do not only resemble the models used by theorists to study prominence formation and support (the KS and KR models) but also provide a mechanism for their development (which has previously been lacking).

The gravitational scale height is too small compared to the prominence height for plasma pressure alone to hold up the material [29], and since the magnitude of the Lorentz force is directly proportional to the curvature of the field lines, dips in the lines are considered by many to be necessary for the magnetic field to support the plasma against gravity. It could even be possible that if the flux escapes the photosphere with the dips already formed, then they could trap and lift the photospheric plasma to form the prominence; however, this would require further research with time-dependent models. The models derived in this paper certainly have many concave up field lines, along with current sheets, that could trap plasma. Many of the diagrams have both features present at once.

The structures also have many places where the field lines descend into the downward flow of the convection cell. Plasma following these lines could form the feet

that connect the prominence to the photosphere. The topologies also have enough variation to provide the fibril structure observed in nature.

Future work in this area could go in many directions – towards actual prominence formation for example. The field lines derived here could be superimposed on an atmosphere with a given density distribution (creating high or low plasma β 's) and the thermodynamics of the resulting prominences studied. The next phase of my research study will be to wave motion in plasmas. In a series of papers, Roberts along with Edwin and Joarder [46, 47, 27] studied wave propagation and oscillation modes in simple magnetic configurations, such as slabs and cylinders. The same could be done with the models developed here. With the lack of exact solutions the dispersion relation would have to be obtained numerically, but it would be interesting to see which MHD modes survive and propagate. This could provide an explanation as to why prominences suddenly erupt. Certain magnetoacoustic modes, for example, may upset the equilibrium of the prominence.

The propagation of magnetoacoustic-gravity waves in a magnetoatmosphere structured by the fields derived here could also be studied. Adam [48, 49, 9] and McKaig and Adam [50] treated such waves in an atmosphere with an imposed horizontal magnetic field. This work could be continued in the context of prominence theory.

As we learn more about the Sun's atmosphere from satellites such as SOHO we see more phenomena for the field of applied mathematics to model. The detail seen by these instruments reveals structures and flows that will keep the student of MHD busy for many years to come.

BIBLIOGRAPHY

- [1] J.A. Adam, "Non-Radial stellar oscillations: A perspective from potential scattering", *Astrophysics and Space Science* 220, 179 (1994)
- [2] R.B. Leighton, R.W. Noyes and G.W. Simon, "Velocity fields in the solar atmosphere I. Preliminary report", *ApJ* 135, 474 (1962)
- [3] A.H. Nye and J.H. Thomas, "Solar magneto-atmospheric waves. II. A model for running penumbral waves", *ApJ* 204, 582 (1976)
- [4] E.N. Parker, *Cosmical Magnetic Fields, their origin and activity*, Oxford University Press, Oxford, England (1979)
- [5] E.R. Priest, *Solar Magnetohydrodynamics*, D. Reidel Publ. Co., Dordrecht, Holland (1982)
- [6] T.G. Cowling, *Magnetohydrodynamics*, Adam Hilger Ltd., Bristol, England (1976)
- [7] V.C.A. Ferraro and C. Plumpton, "Hydromagnetic waves in a horizontally stratified atmosphere", *ApJ* 127, 459 (1958)
- [8] J.H. Thomas, "Magneto-atmospheric waves", *Ann. Rev. Fluid Mech.* 15, 321 (1983)
- [9] J.A. Adam, "An initial value problem for magnetoatmospheric waves: I. Theory", *Wave Motion* 12, 385 (1990)

- [10] M.S. Howe, "On gravity-coupled magnetohydrodynamic waves in the sun's atmosphere", *ApJ* 156, 27 (1969)
- [11] R. Erdélyi, "Resonant absorption of Alfvén waves in steady coronal loops", *Solar Phys.* 180, 213 (1997)
- [12] L.M.B.C. Campos, "On waves in gases. Part II: Interaction of sound with magnetic and internal modes", *Rev. Mod. Phys.* 59, 363 (1987)
- [13] J.H. Thomas, "The local dispersion relation for magneto-atmospheric waves", *ApJ* 262, 760 (1982)
- [14] P.G. Drazin and W.H. Reid, *Hydrodynamic Stability*, Cambridge University Press, Cambridge (1981)
- [15] S. Chandrasekhar, *Hydrodynamic and Hydromagnetic Stability*, Dover Publications Inc., New York (1961)
- [16] E. Tandberg-Hanssen, "New perspectives on solar prominences", ed. D. Webb et al., *IAU Colloq* 167, 11 (1998)
- [17] H. Zirin, *Astrophysics of the Sun*, Cambridge University Press, Cambridge (1988)
- [18] E. Tandberg-Hanssen, "Physics of solar prominences", ed. E. Jensen et al., *IAU Colloq* 44, 138 (1979)
- [19] L. Ofman and Z. Mouradian, "Are thermal sudden disappearances of prominences driven by resonant absorption of Alfvén waves?", *A&A* 308, 631 (1996)

- [20] E. Tandberg-Hanssen, *Solar Prominences*, D. Reidel Publ. Co., Dordrecht, Holland (1974)
- [21] E.R. Priest, *Dynamics and Structure of Quiescent Solar Prominences*, ed. E.R. Priest, Kluwer Academic Publishers, Dordrecht, Holland (1989)
- [22] E.R. Priest, "Dynamics of Quiescent Prominences", ed. V. Ruždjak et al., *IAU Colloq 117*, 150 (1989)
- [23] R. Kippenhahn and A. Schlüter, "Eine theorie der solaren filamente", *Z. Astrophys 43*, 36 (1957)
- [24] M. Kuperus and M.A. Raadu, "The support of prominences formed in neutral sheets", *A&A 31*, 189 (1974)
- [25] D.H. Menzel, *Proceedings of the Conference on Dynamics of Ionized Media at University College*, London (1951)
- [26] J.W. Dungey, "A family of solutions of the magneto-hydrostatic problem in a conducting atmosphere in a gravitational field", *MNRAS 113*, 180 (1953)
- [27] P.S. Joarder and B. Roberts, "The modes of oscillation of a Menzel prominence", *A&A 273*, 642 (1993)
- [28] U. Anzer, *Dynamics and Structure of Quiescent Solar Prominences*, ed. E.R. Priest, Kluwer Academic Publishers, Dordrecht, Holland (1989)
- [29] P. Démoulin, "New perspectives on solar prominences", ed. D. Webb et al., *IAU Colloq 167*, 78 (1998)

- [30] A. Brown, "On the stability of a hydromagnetic prominence model", *ApJ* 128, 646 (1958)
- [31] A. Poland and U. Anzer, "Energy balance in cool quiescent prominences", *Solar Phys.* 19, 401 (1971)
- [32] J.L. Ballester and E.R. Priest, "A two-dimensional model for a solar prominence", *Solar Phys.* 109, 335 (1987)
- [33] A.M. Milne, E.R. Priest and B. Roberts, "A model for quiescent solar prominences", *ApJ* 232, 304 (1979)
- [34] E.R. Priest, A.W. Hood and U. Anzer, "A twisted flux-tube model for solar prominences. I. General properties", *ApJ* 344, 1010 (1989)
- [35] A.W. Hood and U. Anzer, "A model for quiescent solar prominences with normal polarity", *Solar Phys.* 126, 117 (1989)
- [36] B.C. Low, "Nonisothermal magnetostatic equilibria in a uniform gravity field. II. Sheet models of quiescent prominences", *ApJ* 198, 211 (1975)
- [37] E.N. Parker, "Kinematical hydromagnetic theory and its application to the low solar photosphere", *ApJ* 138, 552 (1963)
- [38] N.O. Weiss, "The expulsion of magnetic flux by eddies", *Proc. Roy. Soc. Lond. A* 293, 310 (1966)
- [39] M.R.E Proctor and N.O. Weiss, "Magnetoconvection", *Rep. Prog. Phys* 45, 1317 (1982)

- [40] N.O. Weiss, *Problems of Stellar Convection*, ed. E.A. Spiegel et al., Springer-Verlag, Berlin, 176 (1977)
- [41] R.V. Churchill and J.W. Brown, *Complex Variables with Applications*, McGraw-Hill Book Co. Inc., NY (1984)
- [42] R. Haberman, *Elementary Applied Partial Differential Equations*, Prentice-Hall Inc., NJ (1998)
- [43] R. Burden, J. Faires, and A. Reynolds, *Numerical Analysis*, Prindle, Weber and Schmidt, Boston (1978)
- [44] I. McKaig, "A Dirichlet problem with applications to solar prominences", *A&A* 368, 280 (2001)
- [45] I. McKaig, "Solar prominence magnetic configurations derived numerically from convection", *A&A* 371, 328 (2001)
- [46] B. Roberts, "Wave propagation in a magnetically structured atmosphere. II. Waves in a magnetic slab", *Solar Phys.* 69, 39 (1981)
- [47] P.M. Edwin and B. Roberts, "Wave propagation in a magnetic cylinder", *Solar Phys.* 88, 179 (1983)
- [48] J.A. Adam, "Solar magnetoatmospheric waves—a simplified mathematical treatment", *A&A* 60, 171 (1977)
- [49] J.A. Adam, "A nonlinear eigenvalue problem in astrophysical magnetohydrodynamics: Some properties of the spectrum", *J. Math. Phys.* 30, 744 (1988)

- [50] I. McKaig and J.A. Adam, "Propagation of magnetoacoustic-gravity waves in a horizontally- stratified medium: IV. Kinematics", *Astrophysics and Space Science* **202**, 259 (1993)

APPENDIX A

THE METHOD OF IMAGES

The infinite space Green's function satisfies the Poisson equation $\nabla^2 G(x, y; x_0, y_0) = \delta(x - x_0, y - y_0)$ and the solution G gives the effect at (x, y) of a concentrated source at (x_0, y_0) . If we let r be the distance from (x, y) to (x_0, y_0) and assume that G depends only on r , then away from (x_0, y_0) we have $\nabla^2 G(r) = 0$ where $r = \sqrt{(x - x_0)^2 + (y - y_0)^2}$. Writing the Laplacian in cylindrical coordinates gives:

$$\frac{1}{r} \frac{d}{dr} \left(r \frac{dG}{dr} \right) = 0,$$

which can be solved by integration to get $G(r) = c_1 \ln r + c_2$.

Now, since $\nabla^2 G = \delta(x - x_0, y - y_0)$ at $r = 0$ we can use the the sifting property of the delta function, along with the divergence theorem to find:

$$\iint_C \nabla^2 G dA = 1 \Rightarrow \oint_{\partial C} \nabla G \cdot \hat{n} ds = 1,$$

where C is a circle centered on (x_0, y_0) . Since G only depends on r , which is constant on the circle, we find $2\pi r \frac{dG}{dr} = 1$ so $c_1 = \frac{1}{2\pi}$. Setting $c_2 = 0$ for convenience gives the infinite space Green's function:

$$G(x, y; x_0, y_0) = \frac{1}{2\pi} \ln \sqrt{(x - x_0)^2 + (y - y_0)^2}.$$

Using the method of images we can use this to find an infinite space Green's function that satisfies $G = 0$ on $y = 0$. We let $\nabla^2 G = \delta(x - x_0, y - y_0) - \delta(x - x_0, y + y_0)$

then, at $y = 0$, the response from (x_0, y_0) and $(x_0, -y_0)$ being equal and opposite will cancel, forcing G to be 0 along $y = 0$. Since this equation is linear we have by superposition:

$$\begin{aligned} G(x, y; x_0, y_0) &= \frac{1}{2\pi} \ln \sqrt{(x - x_0)^2 + (y - y_0)^2} - \frac{1}{2\pi} \ln \sqrt{(x - x_0)^2 + (y + y_0)^2} \\ &= \frac{1}{4\pi} \ln \frac{(x - x_0)^2 + (y - y_0)^2}{(x - x_0)^2 + (y + y_0)^2}. \end{aligned}$$

We can now use Green's formula and the symmetry of G (i.e. $G(x, y; x_0, y_0) = G(x_0, y_0; x, y)$) to solve Laplace's equation $\nabla^2 A(x, y) = 0$ subject to $A(x, 0) = h(x)$ on the half-plane $-\infty < x < \infty, y > 0$:

$$\begin{aligned} \int_0^{\infty} \int_{-\infty}^{\infty} A \nabla^2 G - G \nabla^2 A \, dx dy &= \oint (A \nabla G - G \nabla A) \cdot (-j) \, ds \\ &= \int_{-\infty}^{\infty} \left(G \frac{\partial A}{\partial y} - A \frac{\partial G}{\partial y} \right) \Big|_{y=0} \, dx. \end{aligned}$$

Using the boundary conditions for A and G , and interchanging (x, y) and (x_0, y_0) :

$$\Rightarrow A(x, y) = - \int_{-\infty}^{\infty} h(x_0) \frac{\partial G}{\partial y_0} \Big|_{y_0=0} \, dx_0 = \frac{1}{\pi} \int_{-\infty}^{\infty} h(x_0) \frac{y}{(x - x_0)^2 + y^2} \, dy_0.$$

APPENDIX B

THE MATHEMATICA CODE

Here is the Mathematica code used to create the figures in the last section.

First define the box and the stepsize:

```
a = -6.3; b = 6.3; c = -4.; d = 4.;  
n = 40; m = 40; h =  $\frac{b-a}{n}$ ; k =  $\frac{d-c}{m}$ ;  
x = Table[a + i h, {i, 1, n - 1}];  
y = Table[c + i k, {i, 1, m - 1}];
```

Now for the stream function and the velocity potential:

```
 $\Psi[x_, y_] := -\text{Sin}[x]\text{Exp}[-y]$   
 $\phi[x_, y_] := -\text{Cos}[x]\text{Exp}[-y]$   
 $v1[x_, y_] := \text{Sin}[x]\text{Exp}[-y]$   
 $v2[x_, y_] := \text{Cos}[x]\text{Exp}[-y]$   
 $v1x[x_, y_] := \text{Cos}[x]\text{Exp}[-y]$   
 $v2y[x_, y_] := -\text{Cos}[x]\text{Exp}[-y]$ 
```

Set the magnetic diffusivity η , define the functions $f(x,y)$ and $g(x,y)$, and fill matrix

A with zero's:

```
 $\eta = 1;$   
 $f[x_, y_] := \text{If}[y \leq 0, 0.25(2(v1x[x, y] + v2y[x, y]) - \frac{1}{\eta}(v1[x, y]^2 + v2[x, y]^2)), 0];$   
 $g[x_, y_] := \frac{(h k)^2}{\eta} f[x, y] - 2(h^2 + k^2)$   
A = Table[0, {i, 1, (n - 1)(m - 1)}, {j, 1, (n - 1)(m - 1)}];
```

Now to define the coefficient matrix:

first the four corners:

$$A[[1, 1]] = g[x[[1]], y[[1]]]; \quad A[[1, 2]] = k^2; \quad A[[1, n]] = h^2;$$

$$A[[n - 1, n - 1]] = g[x[[n - 1]], y[[1]]];$$

$$A[[n - 1, n - 2]] = k^2; \quad A[[n - 1, 2n - 2]] = h^2;$$

$$A[[m - 2)(n - 1) + 1, (m - 2)(n - 1) + 1]] = g[x[[1]], y[[m - 1]]];$$

$$A[[m - 2)(n - 1) + 1, (m - 2)(n - 1) + 2]] = k^2;$$

$$A[[m - 2)(n - 1) + 1, (m - 2)(n - 1) + 2 - n]] = h^2;$$

$$A[[m - 1)(n - 1), (m - 1)(n - 1)]] = g[x[[n - 1]], y[[m - 1]]];$$

$$A[[m - 1)(n - 1), (m - 1)(n - 1) - 1]] = k^2;$$

$$A[[m - 1)(n - 1), (m - 2)(n - 1)]] = h^2;$$

now the four sides:

For $[i = n; j = 2, j \leq m - 2, i = i + n - 1; j ++,$

$$A[[i, i]] = g[x[[1]], y[[j]]];$$

$$A[[i, i + 1]] = k^2;$$

$$A[[i, i - (n - 1)]] = h^2;$$

$$A[[i, i + (n - 1)]] = h^2]$$

For $[i = 2n - 2; j = 2, j \leq m - 2, i = i + n - 1; j ++,$

$$A[[i, i]] = g[x[[n - 1]], y[[j]]];$$

$$A[[i, i - 1]] = k^2;$$

$$A[[i, i - (n - 1)]] = h^2;$$

$$A[[i, i + (n - 1)]] = h^2]$$

For $[i = 2, i \leq n - 2, i ++,$

$$A[[i, i]] = g[x[[i]], y[[1]]];$$

$$A[[i, i - 1]] = k^2;$$

$$A[[i, i + 1]] = k^2;$$

$$A[[i, i + (n - 1)]] = h^2]$$

For $[i = (m - 2)(n - 1) + 2; j = 2, i \leq (m - 1)(n - 1) - 1, i ++; j ++,$

$$A[[i, i]] = g[x[[j]], y[[m - 1]]];$$

$$A[[i, i - 1]] = k^2;$$

$$A[[i, i + 1]] = k^2;$$

$$A[[i, i - (n - 1)]] = h^2]$$

Now for the interior:

For[$i = 2, i \leq n - 2, i ++$,

For[$j = 2, j \leq m - 2, j ++, \xi = i + (j - 1)(n - 1)$;

$$A[[\xi, \xi]] = g[x[[i]], y[[j]]];$$

$$A[[\xi, \xi - 1]] = k^2;$$

$$A[[\xi, \xi + 1]] = k^2;$$

$$A[[\xi, \xi - (n - 1)]] = h^2;$$

$$A[[\xi, \xi + (n - 1)]] = h^2];$$

Now for the boundary conditions:

$$g1[y_-] := 0$$

$$g2[y_-] := 0$$

$$h1[x_-] := 100$$

$$h2[x_-] := 0$$

$$B = \text{Table}[0, \{i, 1, (n - 1)(m - 1)\}]; B[[1]] = h^2 h2[x[[1]]] + k^2 g2[y[[1]]];$$

$$B[[n - 1]] = h^2 h2[x[[n - 1]]] + k^2 g1[y[[1]]];$$

$$B[[m - 2, (n - 1) + 1]] = h^2 h1[x[[1]]] + k^2 g2[y[[m - 1]]];$$

$$B[[m - 1, (n - 1)]] = h^2 h1[x[[n - 1]]] + k^2 g1[y[[m - 1]]];$$

$$\text{For}[i = n; j = 2, j \leq m - 2, i = i + n - 1; j ++, B[[i]] = k^2 g2[y[[j]]];$$

$$\text{For}[i = 2n - 2; j = 2, j \leq m - 2, i = i + n - 1; j ++, B[[i]] = k^2 g1[y[[j]]];$$

$$\text{For}[i = 2, i \leq n - 2, i ++, B[[i]] = h^2 h2[x[[i]]];$$

$$\text{For}[i = (m - 2)(n - 1) + 2; j = 2, i \leq (m - 1)(n - 1) - 1, i ++; j ++,$$

$$B[[i]] = h^2 h1[x[[j]]];$$

Lets get the solution, combine it with the stream function and save it:

```

 $\Lambda = \text{Partition}[\text{LinearSolve}[A, -B], n - 1];$ 
 $\Omega = \text{Table}[\Lambda[[i, j]] \text{Exp}[\frac{\phi[x[[j]], y[[i]]}{2\eta}], \{i, 1, m - 1\}, \{j, 1, n - 1\}];$ 
 $p1 = \text{ListContourPlot}[\Omega, \text{ContourShading} \rightarrow \text{False}, \text{Contours} \rightarrow 50,$ 
     $\text{MeshRange} \rightarrow \{\{a, b\}, \{c, d\}\};$ 
 $p2 = \text{ContourPlot}[\Psi[x, y], \{x, a, b\}, \{y, c, 0\}, \text{ContourShading} \rightarrow \text{False},$ 
     $\text{Contours} \rightarrow 30, \text{PlotPoints} \rightarrow 100, \text{ContourStyle} \rightarrow \text{GrayLevel}[0.5]]$ 
 $\text{Show}[p1, p2];$ 
 $\text{Export}["figure.eps", \%];$ 

```


APPENDIX C

PERMISSION TO USE COPYRIGHTED MATERIAL

I would like to thank Dr. Denker of Big Bear Solar Observatory and Dr. Charbonneau of the High Altitude Observatory for permission to use slides from their websites. Slides were also used from the website of the Solar and Heliospheric Observatory with appropriate credit given.

I should also thank Dr. Weiss for his permission to use a figure from one of his papers on flux expulsion, and Dr. Bertout (Editor-in-Chief of *Astronomy and Astrophysics*) for allowing me to use my papers published in that journal.

From: Carsten Denker <cdenker@bbso.njit.edu>
To: Iain McKaig <tcmkai@tc.cc.va.us>
Date: 2/27/01 12:09PM
Subject: Re: Use of pictures

Dear Iain:

Please feel free to use these images as long as put somewhere a proper credit line (Big Bear Solar Observatory/NewJersey Institute of Technology). If it's not too much work for you, we would also appreciate a sample copy.

Ciao,
 Carsten

```

+-----+
|                               |
| Dr. Carsten Denker           |
|                               |
| Big Bear Solar Observatory   Tel.: 909-866-5791 Ext. 13   |
| 40386 North Shore Lane     FAX: 909-866-4240           |
| Big Bear City               E-Mail: cdenker@bbso.njit.edu   |
| CA 92314-9672, U.S.A.      WWW: http://www.bbso.njit.edu/~cdenker/ |
|                               |
+-----+

```

From: Paul Charbonneau <paulchar@hao.ucar.edu>
To: "Iain McKaig" <tcmkai@tc.cc.va.us>
Date: 3/5/01 3:23PM
Subject: Re: Use of slides

Greetings Iain. You may use all slides from 6 to 10 for your thesis, with appropriate credit to HAO/NCAR. Good luck with the dissertation writing.


Paul Charbonneau, HAO/NCAR

Copyright Notice

Use of SOHO images for public education efforts and non-commercial purposes is strongly encouraged and requires no expressed authorization. It is requested, however, that any such use properly attribute the source of the images as:

"Coverage of SOHO's Environment near the Sun from STEREO is a project of international cooperation between ESA and NASA."

Below is the instrument that provided the images:



Source/Credits: Solar & Heliospheric Observatory (SOHO). STEREO is a project of international cooperation between ESA and NASA.

From: Nigel Weiss <N.O.Weiss@damtp.cam.ac.uk>
To: Iain McKaig <tcmkai@tc.cc.va.us>
Date: 3/1/01 7:59AM
Subject: Re: Use of figures

Dear Iain

You are welcome to use those figures in your paper. I am glad that they are still proving useful!

Since then there have been other investigations of flux expulsion. The 2D problem was studied by Tao et al. (MNRAS 300, 907-914, 1998) and there is a much more ambitious 3D calculation that is about to appear in Ap.J. You could get hold of it by contacting Steve Tobias at Leeds (his email address is smt@amsta.leeds.ac.uk).

Best wishes

Nigel Weiss

Professor N.O. Weiss
D.A.M.T.P. Phone: (+44) 1223 337910
Silver Street Fax: (+44) 1223 337918
Cambridge CB3 9EW, U.K. email: now@damtp.cam.ac.uk

From: "Claude Bertout" <bertout@iap.fr>
To: "Iain McKaig (by way of JournalA&A <aanda@obspm.fr>)" <tcckai@tc.cc.va.us>
Date: 3/13/01 1:00PM
Subject: Re: Permission to use material in H2492 and H2648

Dear Mr. McKaig,

You are hereby permitted to use in your dissertation the A&A papers mentioned below.

With my best wishes for you thesis defense.
 Yours sincerely

Claude Bertout
 Editor-in-Chief
 Copyright holder for A&A

----- Original Message -----

From: "Iain McKaig (by way of JournalA&A <aanda@obspm.fr>)" <tcckai@tc.cc.va.us>
To: <claude.bertout@obspm.fr>
Sent: Tuesday, March 13, 2001 9:19 AM
Subject: Permission to use material in H2492 and H2648

> Dear Dr. Bertout,
 >
 > My name is Iain McKaig and I teach mathematics at Tidewater Community
 > College in Virginia Beach VA. Currently I am working on my Ph.D. in
 > applied mathematics at Old Dominion University in Norfolk VA. To this end
 > I have published two papers in A&A, H2492 - "A Dirichlet Problem with
 > Applications to Solar Prominences" and H2648 - "Solar Prominence Magnetic
 > Configurations Derived Numerically from Convection."
 >
 > It is my understanding that I need your permission to use these papers in
 > my dissertation. If you could grant me this permission I would greatly
 > appreciate it. Other than obtaining my degree I will not profit in any
 > way
 > from this thesis.
 >
 > Thanks for your consideration of this request, and I look forward to
 > sending A&A more papers in the future.
 >
 > Best Regards
 > Iain McKaig
 >

VITA

Iain McKaig was born in Dunfermline Scotland in 1963, moving to the States in 1979 via Malta, Mauritius and London, England. In 1984 he received a Bachelor of Arts in Mathematics and Computer Science from Virginia Wesleyan College in Virginia Beach, Virginia, graduating magna cum laude. After waiting tables and then working as a systems analyst, he earned a Master of Science in Computational and Applied Mathematics at Old Dominion University in 1990. He will obtain a Doctorate in Computational and Applied Mathematics in December 2001.

Mr. McKaig has worked for the past ten years as a teacher of mathematics at Tidewater Community College in Virginia Beach, Virginia, rising through the ranks from Instructor to Associate Professor. With the completion of his Ph.D. he hopes to finally obtain the status of full Professor by August of 2002.

Publications:

Propagation of Magnetoacoustic-Gravity Waves in a Horizontally-Stratified Medium: IV. Kinematics, Astrophysics and Space Science, 202: 259-271, 1993. Co-authored by Dr. J. A. Adam.

Scattering from Stellar Acoustic-Gravity Potentials: II. Phase Shifts via the First Born Approximation, Applied Math. Letters, 10, No. 3: 39-42, 1997. Co-authored by Dr. J. .A. Adam.

A Dirichlet Problem with Applications to Solar Prominences, Astronomy and Astrophysics, 368: 280-284, 2001.

Solar Prominence Magnetic Configurations Derived Numerically from Convection, Astronomy and Astrophysics, 371: 328-332, 2001

This document was prepared by the author using L^AT_EX 2_ε